IMPLEMENTATION OF A NEWTON-BASED OPTIMAL POWER FLOW INTO A POWER SYSTEM SIMULATION ENVIRONMENT

BY

JAMES DANIEL WEBER

B.S., University of Wisconsin - Platteville, 1995

THESIS

Submitted in partial fulfillment of the requirements
for the degree of Master of Science in Electrical Engineering
in the Graduate College of the
University of Illinois at Urbana-Champaign, 1997

Urbana, Illinois

RED-BORDERED FORM

ABSTRACT

In this thesis, a Newton-based optimal power flow (OPF) is developed for implementation into a power system simulation environment. The OPF performs all system control while maintaining system security. System controls include generator megawatt outputs, transformer taps, and transformer phase shifts, while maintenance of system security ensures that no power system component's limits are violated. Special attention is paid to the heuristics important to creating an OPF which achieves solution in a rapid manner. Finally, sample applications of the OPF are discussed. These include transmission line overload removal, transmission system control, available transfer capability calculation (ATC), real and reactive power pricing, transmission component valuation, and transmission system marginal pricing.

ACKNOWLEDGEMENTS

I would like to thank Professor Thomas Overbye for his knowledge, guidance and support throughout my graduate studies. I would also like to thank the University of Illinois Power Affiliates Program and the University of Illinois Graduate College for their generous financial support.

I would also like to thank my professors and friends from my undergraduate studies while at the University of Wisconsin - Platteville. The preparation and experience I gained there were invaluable. Special thanks go to Dr. Mesut Muslu and Dr. Richard Shultz.

Finally, I would like to thank my family. My brothers Brian and Scott continue to be there for support and friendship. Most of all I thank my mother and father, Jan and Gene. They continue to supply the unconditional love and support which allow me and my brothers to achieve what we have and will.

TABLE OF CONTENTS

LIST OF TABLES

Table Page

LIST OF FIGURES

Figure Page

NOTATION

Throughout this thesis, variables that do not have a subscript next to them may be considered vectors or matrices, while all variables that refer to a scalar will have a subscript next to them.

V_k	Magnitude of voltage at bus k.
δ_k	Angle of voltage at bus k.
t_{km}	Transformer tap ratio between buses k and m.
α_{km}	Transformer phase shift between buses k and m.
P_{Gk}	The real power generated at bus k.
b_{km}	Element of the imaginary part of the network admittance matrix.
g_{km}	Element of the real part of network admittance matrix.
y_{km}	Magnitude of an element of the network admittance matrix.
δ_{km}	Phasor angle of an element of the network admittance matrix.
P_k	Real power injection at bus k.
Q_k	Reactive power injection at bus k.
P_{km}	The real power flow from bus k to bus m.
Q_{km}	The reactive power flow from bus k to bus m.
S_{km}	The MVA flow from bus k to bus m.
P_{int}	The real power interchange for an area.
P_{sched}	The scheduled real power interchange for an area.
$f(\bullet)$	The objective function.
$g(\bullet)$	Equality constraints.
$h(\bullet)$	Inequality constraints.
L(•)	The Lagrange function or Lagrangian.
H(•)	The Hessian of the Lagrangian.
∇L(•)	The gradient of the Lagrangian.
a_i, b_i, and c_i,	Coefficients for the quadratic cost curve of a generator
X_{max}	Signifies a maximum bound on a variable.

X_{min}	Signifies a minimum bound on a variable.
μ	In general, this is a Lagrange multiplier for an equality constraint.
λ	In general, this is a Lagrange multiplier for an inequality constraint.

List of Lagrange multipliers

μ_{Pk}	For P_k, the real power injection at bus k.
μ_{Qk}	For Q_k, the reactive power injection at bus k.
μ_{viset}	For generator voltage set point.
μ_{int}	For generator voltage set point.
λ_{Skm}	For MVA constraint on line from bus k to m.
λ_{PGih}	For generator maximum power output constraint at bus i.
λ_{PGil}	For generator minimum power output constraint at bus i.
λ_{Vih}	For maximum bus voltage constraint at bus i.
λ_{Vil}	For minimum bus voltage constraint at bus i.
$\lambda_{tkm\ max}$	For maximum transformer tap ratio constraint .
$\lambda_{tkm\ min}$	For minimum transformer tap ratio constraint.
$\lambda_{\alpha km\ max}$	For maximum transformer phase shift constraint.
$\lambda_{\alpha km\ min}$	For minimum transformer phase shift constraint.

1. INTRODUCTION

1.1 Motivation

Throughout the entire world, the electric power industry has undergone a considerable change in the past decade and will continue to do so for the next several decades. In the past the electric power industry has been either a government-controlled or a government-regulated industry which existed as a monopoly in its service region. All people, businesses, and industries were required to purchase their power from the local monopolistic power company. This was not only a legal requirement, but a physical engineering requirement as well. It just didn't appear feasible to duplicate the resources required to connect everyone to the power grid.

Over the past decade, however, countries have begun to split up these monopolies in favor of the free market. Numerous papers and articles have been written on this topic with a good overview of the topic found in a series of articles written for IEEE Spectrum in July and August of 1996 [1 - 6]. In the United States, the change from the regulated monopoly to the free market system has become known as restructuring. For the remainder of this thesis, it will be referred to as restructuring.

One of the cornerstones of any restructuring plan is the ability to operate the transmission system in a manner which is fair to all participants in the industry. In the United States, the Federal Energy Regulatory Commission (FERC) oversees issues involving the transmission system. FERC presently believes that the only manner in which everyone will be on an equal playing field is to create open access to all. As stated in [7], "participants in wholesale power markets will have non-discriminatory open access to the transmission systems of public utilities."

In order to achieve the ideal of open access, many outstanding engineering problems will need to be investigated and tools created for their solution.

It is very important that these problems be addressed early in the restructuring process. If these engineering problems become overshadowed by short term economic concerns, then the result could be decreased electricity reliability. In the past year, the western United States has seen the consequences of pushing the transmission system too hard on two separate occasions. The two multistate blackouts in the Western States Coordinating Council (WSCC) system in the last several months may be destined to repeat themselves [8].

In a presently unpublished report from a joint PSERC/EPRI workshop, many of these tools were identified [9]. A partial list of problems that can be addressed from the work done in this thesis follows:

Control Problems

- Computation of real-time available transfer capability (ATC)
- Real-time control of power flows
- Tools to relieve congestion in fair, justifiable and economic manner
- Tools for congestion management (including congestion pricing)
- Tools for determining the ISO action before the contingency occurs

Economic Problems

- Real-time pricing and price risk management services
- Tools for operating the power system in the most economical manner
- Transaction evaluation tools that enable players to evaluate their own costs
- Methodologies for determining the value (cost) of ancillary services in improving efficiency and flexibility

User-Interface and Simulation Problems

- Market simulation models
- Better tools for communication and display of information will permit the better operation of the min ISO scenario

The work presented in this thesis utilizes an optimal power flow program, OPF, as the tool for solving these problems. The OPF is a natural choice for addressing these concerns because it is basically an optimal control problem. The OPF utilizes all control variables to help minimize the costs of the power system operation. It also yields valuable economic information and insight into the power system. In these ways, the OPF very adeptly addresses both the control and economic problems.

After creating the OPF program, the user-interface and simulation problems may also be addressed by implementing the OPF into a power system simulator. In this way, the results of the economic and control operations of the OPF can easily be utilized by the user of the program.

1.2 Literature Survey

The optimal power flow problem has been discussed since its introduction by Carpentier in 1962 [10]. Because the OPF is a very large, non-linear mathematical programming problem, it has taken decades to develop efficient algorithms for its solution. Many different mathematical techniques have been employed for its solution. The majority of the techniques discussed in the literature use one of the following five methods [11, p.517]:

- Lambda iteration method - Also called the equal incremental cost criterion (EICC) method. This method has its roots in the common method of economic dispatch used since the 1930s. See [11, p. 39]
- Gradient method - See paper written by Dommel and Tinney [12]
- Newton's method - See paper by Sun et al. [13]
- Linear programming method - See paper by Alsac et al. [14]
- Interior point method - See paper by Wu, Debs, and Marsten [15]

An excellent literature survey of the different techniques can be found in a paper by Huneault and Galieana published in 1991 [16]. Though it does not discuss the interior point method, it does make reference to over 150 papers on the optimal power flow problem covering all the other methods for solving the OPF.

This thesis will explore the application of Newton's method to the OPF problem. Specifically, it will explore the implementation of a Newton's method based OPF in the power system simulator POWERWORLD [17].

1.3 Goals of the OPF

Before beginning the creation of an OPF, it is useful to consider the goals that the OPF will need to accomplish. The primary goal of a generic OPF is to minimize the costs of meeting the load demand for a power system while maintaining the security of the system. The costs associated with the power system may depend on the situation, but in general they can be attributed to the cost of generating power (megawatts) at each generator. From the viewpoint of an OPF, the maintenance of system security requires keeping each device in the power system within its desired operation range at steady-state. This will include maximum and minimum outputs for generators, maximum MVA flows on transmission lines and transformers, as well as keeping system bus voltages within specified ranges. It should be noted that the OPF only addresses steady-state operation of the power system. Topics such as transient stability, dynamic stability, and steady-state contingency analysis are not addressed.

To achieve these goals, the OPF will perform all the steady-state control functions of the power system. These functions may include generator control and transmission system control. For generators, the OPF will control generator MW outputs as well as generator voltage. For the transmission system, the OPF may control the tap ratio or phase shift angle for variable transformers, switched shunt control, and all other flexible ac transmission system (FACTS) devices.

A secondary goal of an OPF is the determination of system marginal cost data. This marginal cost data can aid in the pricing of MW transactions as well as the pricing ancillary services such as voltage support through MVAR support. In solving the OPF using Newton's method, the marginal cost data are determined as a by-product of the solution technique. This will be discussed later in Section 2.4 on page 22.

1.4 Overview

The OPF program written in conjunction with this thesis uses Newton's method as its solution algorithm. It will tackle all of the goals set forth for an OPF except the control of switched shunts and other FACTS devices. The control of these may be added at a later time as desired.

The remainder of this thesis will discuss the development of the OPF. Chapter 2 of this thesis will discuss the theory of the Newton-based optimal power flow. It will lay a framework for the mathematics and engineering behind the OPF computer source code. Chapter 3 will discuss some special heuristics important to creating an OPF which achieves solution in a rapid manner. Chapter 4 will show several sample applications of the OPF. The sample applications

discussed will include transmission line overload removal, transmission system control, available transfer capability (ATC) calculations, real and reactive power pricing, transmission component valuation, and transmission system marginal pricing. Finally, Chapter 5 will conclude with a summary and several improvements which would aid in creating a truly useful OPF.

2. DEVELOPMENT OF NEWTON-BASED OPTIMAL POWER FLOW

2.1 Background on Newton's Method

Newton's method is well-known in the area of power systems. It has been the standard solution algorithm for the power flow problem for decades [18]. A good reference for the theory of Newton's method is a book by Luenberger [19], which describes Newton's method as well as its quadratic convergence properties. The detailed explanation in [19] is left to the interested reader. This thesis will only cover the process of applying Newton's method to a minimization problem such as the OPF.

Newton's method is a very powerful solution algorithm because of its rapid convergence near the solution. This property is especially useful for power system applications because an initial guess near the solution is easily attained. System voltages will be near rated system values, generator outputs can be estimated from historical data, and transformer tap ratios will be near 1.0 p.u.

2.1.1 Problem statement

A general minimization problem can be written in the following form.

Minimize	$f(x)$		(the objective function)
subject to:	$h_i(x) = 0,$	$i = 1, 2, \ldots, m$	(equality constraints)
	$g_j(x) \leq 0,$	$j = 1, 2, \ldots, n$	(inequality constraints)

There are m equality constraints and n inequality constraints and the number of variables is equal to the dimension of the vector x.

2.1.2 Development of Lagrangian, gradient and Hessian

The solution of this problem by Newton's method requires the creation of the Lagrangian as shown below.

$$L(z) = f(x) + \mu^T h(x) + \lambda^T g(x) \quad = \quad \text{the Lagrangian}$$

where $z = \begin{bmatrix} x & \mu & \lambda \end{bmatrix}^T$, μ and λ are vectors of the Lagrange multipliers, and *g(x)* only includes the active (or binding) inequality constraints.

A gradient and Hessian of the Lagrangian may then be defined.

$$\text{Gradient} = \nabla L(z) = \left[\frac{\partial L(z)}{\partial z_i}\right] \quad = \text{a vector of the first partial derivatives of the Lagrangian}$$

$$\text{Hessian} = \nabla^2 L(z) = H = \left[\frac{\partial^2 L(z)}{\partial z_i \partial z_j}\right] = \begin{bmatrix} \frac{\partial^2 L(z)}{\partial x_i \partial x_j} & \frac{\partial^2 L(z)}{\partial x_i \partial \mu_j} & \frac{\partial^2 L(z)}{\partial x_i \partial \lambda_j} \\ \frac{\partial^2 L(z)}{\partial \mu_i \partial x_j} & 0 & 0 \\ \frac{\partial^2 L(z)}{\partial \lambda_i \partial x_j} & 0 & 0 \end{bmatrix} = \quad \begin{array}{l} \text{a matrix of the} \\ \text{second partial} \\ \text{derivatives of} \\ \text{the Lagrangian} \end{array}$$

Note the extremely sparse structure of the Hessian matrix shown. This sparsity will be exploited in the solution algorithm.

From this, according to optimization theory, the Kuhn-Tucker necessary conditions of optimality are [19, p. 314]:

$\nabla_x L(z^*) = \nabla_x L([x^*, \lambda^*, \mu^*]) = 0;$
$\nabla_\lambda L(z^*) = \nabla_\lambda L([x^*, \lambda^*, \mu^*]) = 0;$
$\nabla_\mu L(z^*) = \nabla_\mu L([x^*, \lambda^*, \mu^*]) = 0;$
$\lambda_i^* \geq 0$ if $g(x^*) = 0$ (i.e., the inequality constraint is active)
$\lambda_i^* = 0$ if $g(x^*) \leq 0$ (i.e., the inequality constraint is not active)
μ_i^* = Real

where $z^* = [x^*, \lambda^*, \mu^*]$ is the optimal solution.

Thus solving the equation $\nabla_z L(z^*) = 0$ will yield the optimal problem solution.

2.1.3 Application of inequality constraints

It should be noted that special attention must be paid to the inequality constraints of this problem. As noted, the Lagrangian only includes those inequalities that are being enforced. For example, if a bus voltage is within the desired operating range, then there is no need to activate the inequality constraint associated with that bus voltage. For this Newton's method formulation, the inequality constraints will be handled by separating them into two sets: active and inactive [19, p. 326]. For efficient algorithms, the determination of those inequality constraints that are active is of utmost importance. While an inequality constraint is being enforced, the sign of its associated Lagrange multiplier at solution determines whether continued enforcement of the constraint is necessary. Essentially the Lagrange multiplier is the negative of the derivative of the function that is being minimized with respect to the enforced constraint (see Appendix A for a derivation of this fact). Therefore, if the multiplier is positive, continued enforcement will result in a decrease of the function, and enforcement is thus maintained. If it is negative, then enforcement will result in an increase of the function, and enforcement is thus stopped. The outer loop of the flow chart in Figure 2.1 performs this search for the binding or active constraints.

2.1.4 Solution method

Considering the issues discussed above, the solution of the minimization problem can be found by applying Newton's method to $\nabla_z L(z) = 0$. A flowchart of this process is shown in Figure 2.1. This flowchart will be useful for any generic minimization problem. A more detailed

discussion of this flowchart will be reserved for the following section. There the application of Newton's method to the optimal power flow problem will be discussed.

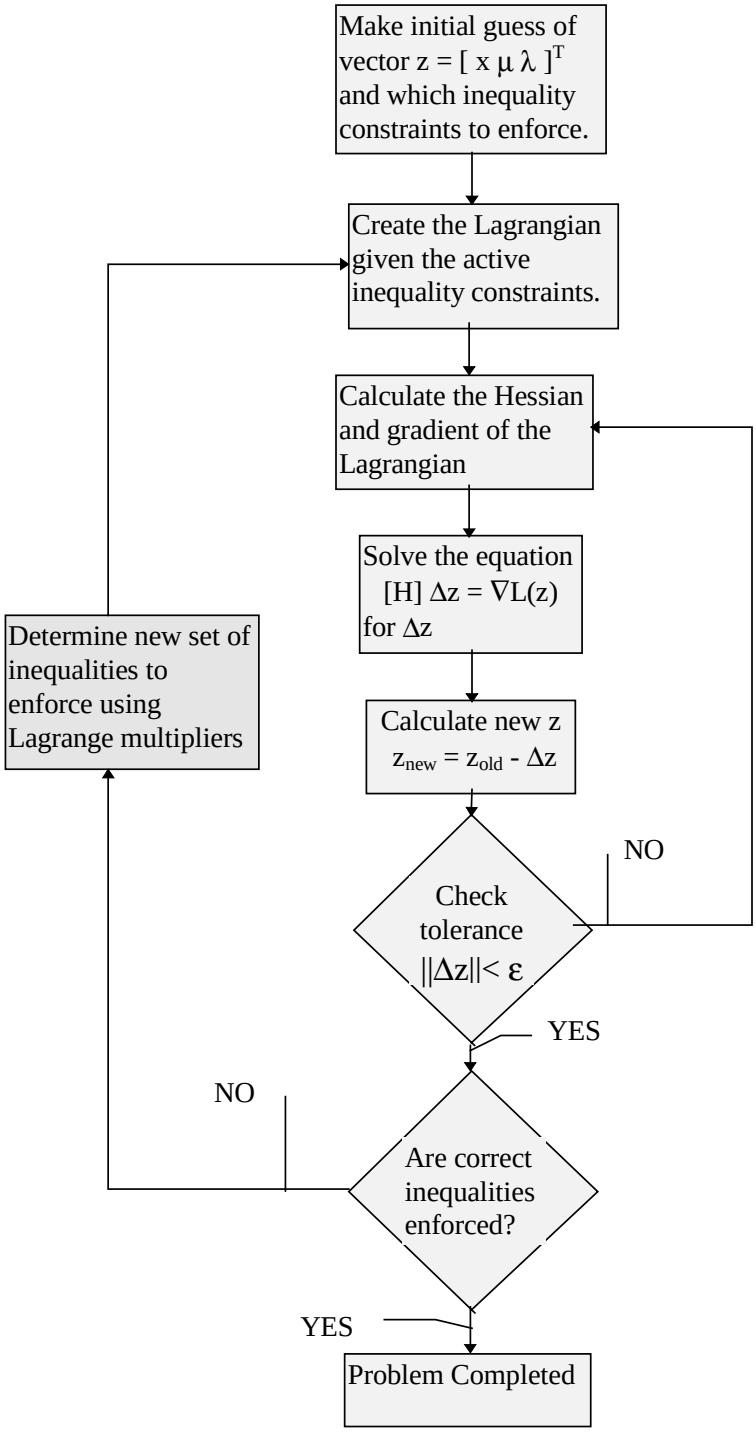

Figure 2.1 Newton's Method Flowchart

2.2 Application of Newton's Method to OPF

As discussed in Section 1.3, the goal of the OPF is to minimize the costs of meeting the load demand for a power system while maintaining the security of the system. This section of the thesis will discuss the application of Newton's method in a manner that will achieve this desired goal.

First, the objective function, *f(x)*, will be introduced. It will reflect the desire to minimize the costs of the system. Then the equality and inequality constraints will be discussed. These constraints model the physical laws of the power system as well as the need to maintain system security. At this point, the concept of soft constraints using penalty functions will be introduced. Penalty functions also model the need to maintain system security. Finally, all terms in the Lagrangian, gradient, and Hessian will be summarized.

2.2.1 The objective function

The objective function for the OPF reflects the costs associated with generating power in the system. The quadratic cost model for generation of power will be utilized:

$$C_{P_{Gi}} = a_i + b_i P_{Gi} + c_i P_{Gi}^{\,2}$$

where P_{Gi} is the amount of generation in megawatts at generator i. The objective function for the entire power system can then be written as the sum of the quadratic cost model at each generator.

$$f(x) = \sum_i \left(a_i + b_i P_{Gi} + c_i P_{Gi}^{\,2} \right)$$

This objective function will minimize the total system costs, and does not necessarily minimize the costs for a particular area within the power system.

2.2.2 Equality constraints

The equality constraints of the OPF reflect the physics of the power system as well as the desired voltage set points throughout the system. The physics of the power system are enforced through the power flow equations which require that the net injection of real and reactive power at each bus sum to zero.

$$P_k = 0 = V_k \sum_{m=1}^{N} \left[V_m \left[g_{km} \cos\left(\delta_k - \delta_m\right) + b_{km} \sin\left(\delta_k - \delta_m\right) \right] \right] - P_{Gk} + P_{Lk}$$

$$Q_k = 0 = V_k \sum_{m=1}^{N} \left[V_m \left[g_{km} \sin\left(\delta_k - \delta_m\right) - b_{km} \cos\left(\delta_k - \delta_m\right) \right] \right] - Q_{Gk} + Q_{Lk}$$

For a derivation of the power flow equations see Grainger and Stevenson [20, p. 330]. For an explanation of forming the network admittance matrix see Grainger and Stevenson [20, p. 33].

It is also common for the power system operators to have voltage set points for each generator. In this case, an equality constraint for each generator is added.

$$V_{Gi} - V_{Gi\,setpo\,\mathrm{int}} = 0$$

Finally, for multiarea power systems, a contractual constraint requires that the net power interchange be equal to the scheduled power interchange. This adds an equality constraint for all but one area.

$$P_{\text{interchange}} - P_{\text{sceduled interchange}} = \sum_{\text{tie lines}} \left[P_{km} \right] - P_{\text{sceduled interchange}} = 0$$

This last area must not have the equality constraint and essentially becomes a “slack area.” Consider a simple three-area system with scheduled interchanges as shown in Figure 2.1. With the loads given and the interchanges constrained for two areas, the last area will be forced to have its interchanges set as planned. Thus, adding another constraint is not needed. Indeed, it will

cause numerical problems if added because the equations associated with this constraint are dependent on the other interchange constraints and would thus lead to a singular Hessian matrix.

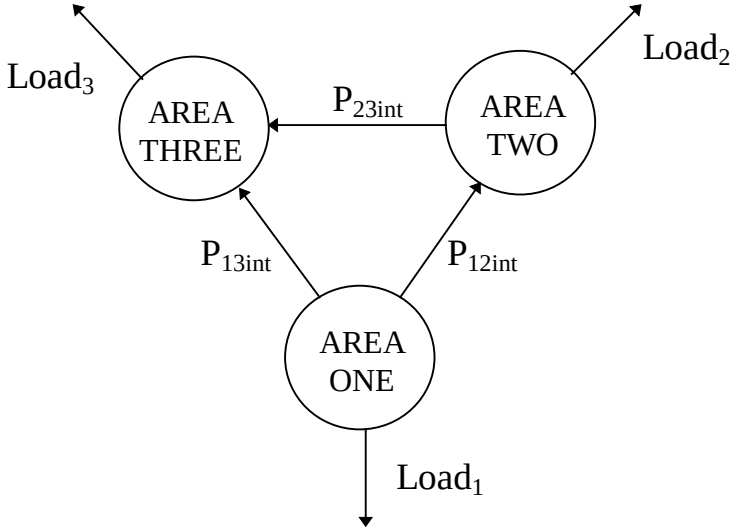

Figure 2.1 Multiarea System with Scheduled Interchanges

2.2.3 Inequality constraints

The inequality constraints of the OPF reflect the limits on physical devices in the power system as well as the limits created to ensure system security. Physical devices that require enforcement of limits include generators, tap changing transformers, and phase shifting transformers. This section will lay out all the necessary inequality constraints needed for the OPF implemented in this thesis.

Generators have maximum and minimum output powers and reactive powers which add inequality constraints.

$$P_{Gi\,\min} \le P_{Gi} \le P_{Gi\,\max}$$
$$Q_{Gi\,\min} \le Q_{Gi} \le Q_{Gi\,\max}$$

Load tap changing transformers have a maximum and a minimum tap ratio which can be achieved and phase shifting transformers have a maximum and a minimum phase shift, which can be achieved. Both of these create inequality constraints.

$$t_{km\,\min} \le t_{km} \le t_{km\,\max}$$

$$\alpha_{km\,\min} \le \alpha_{km} \le \alpha_{km\,\max}$$

For the maintenance of system security, power systems have transmission line as well as transformer MVA ratings. These ratings may come from thermal ratings (current ratings) of conductors, or they may be set to a level due to system stability concerns. The determination of these MVA ratings will not be of concern in this thesis. It is assumed that they are given. Regardless, these MVA ratings will result in another inequality constraint. To make the mathematics less complex, the constraint used in the OPF will limit the square of the MVA flow on a transformer or transmission line.

$$\left|S_{km}\right|^2 - \left|S_{km\,\max}\right|^2 \le 0$$

To maintain the quality of electrical service and system security, bus voltages usually have maximum and minimum magnitudes. These limits again require the addition of inequality constraints.

$$V_{i\,\min} \le V_i \le V_{i\,\max}$$

2.2.4 Soft constraints by using penalty functions

One issue sometimes encountered when trying to solve a minimization problem is the non-existence of a feasible solution. Essentially this means that too many constraints have been added to the problem and no solution exists which obeys all of the constraints. One way to avoid

this issue is to implement soft inequality constraints in the form of penalty functions. The word "soft" signifies that the constraint is not absolutely enforced. The soft constraint only encourages the solution to meet the constraint by enforcing a penalty if the constraint is not met. In the OPF problem, soft equality constraints are not used, because of the nature of the equality constraints in the OPF problem. The power flow equations can not be violated as they are imposed by physics, and the generator set points of a power system are normally not moved around frequently. For the inequality constraints, the penalty functions offer a viable option.

Penalty functions are added to the objective function of the minimization problem. Ideally, a penalty function will be very small near a limit and increase rapidly as the limit is violated more. A well-suited penalty function for use in Newton's method is the quadratic penalty function [19, p. 443] which meets the requirements of a penalty function and is also easily differentiated for use by Newton's method. In the OPF presented in this thesis, soft inequality constraints are available for transmission line MVA limits as well as bus voltage limits.

$$\text{Penalty Functions} \begin{cases} W_{km} = k\left(\left|S_{km}\right|^2 - \left|S_{km\,\max}\right|^2\right)^2 \\ W_i = \begin{cases} k\left(V_{i\,\min} - V_i\right)^2 & ; \quad V_i < V_{i\,\min} \\ 0 & ; \quad V_{i\,\min} \le V_i \le V_{i\,\max} \\ k\left(V_i - V_{i\,\max}\right)^2 & ; \quad V_i > V_{i\,\max} \end{cases} \end{cases}$$

Figure 2.1 and Figure 2.2 show the graphs of these penalty functions used in the OPF.

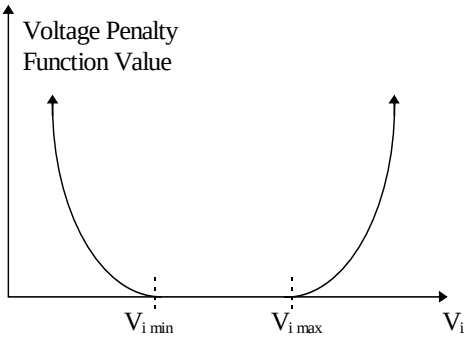

Figure 2.1 Penalty Function for Bus Voltage

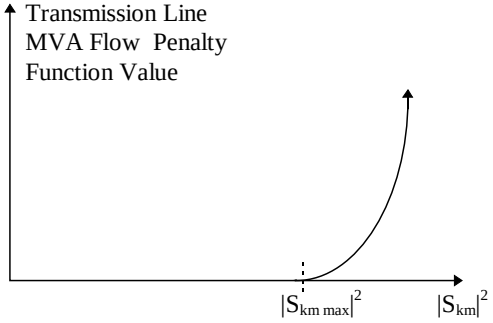

Figure 2.2 Penalty Function for Line MVA Flow Limit

Note that these penalty functions fit the requirements perfectly. While the inequality constraint is not violated, the penalty function has a value of zero. As the constraint begins to be violated, the penalty function quickly increases. Another advantage of the quadratic penalty function is the ability to control how hard or soft to make the constraint. For very large values of k, the quadratic penalty function behaves much like a hard constraint. By adjusting it to smaller values, one can control the importance given to the limit.

After doing trial and error experimentation, values for k were chosen for use in the OPF of this thesis. For soft bus voltage constraints, k was chosen to be $\$200/V^2$. For soft transmission line constraints, k was chosen to be $\$100/MVA^4$.

2.2.5 Treatment of discrete variables

In all the discussions thus far, all variables have been assumed to be continuous. For example, the constraint $V_{i\min} \le V_i \le V_{i\max}$ allows V_i to take on all values within the specified range. The OPF algorithm as presented in this thesis also assumes this for the tap ratios and phase shift angles of variable transformers, although this is not true for them. Variable transformers have a fixed number of discrete tap positions at which they may operate. For example, a typical tap changing transformer has 33 discrete positions (nominal, 16 above and 16 below). This problem should be addressed in future work.

One possible solution for this problem is to round the optimal setting found assuming a continuous tap to the nearest discrete tap. This could be done for all transformers. However, three problems arise from this methodology. First, there is no guarantee that the rounded solution is the optimal solution. Second the solution may become infeasible after rounding, i.e., some constraints may be violated. Finally, this methodology will not work well for discrete variables that have very large step sizes such as switched capacitor banks. This final problem is addressed in references [21, 22].

2.2.6 Summary of optimal power flow problem

In summary, the optimal power flow problem can be written in the following form.

$$\text{minimize:} \quad \sum_{\text{generators}} \left(a_i + b_i P_{Gi} + c_i P_{Gi}^{\,2} \right) \; + \; \sum_{\text{penalties}} \alpha_i$$

$$\text{subject to:} \quad \left.\begin{aligned} P_k &= 0 \\ Q_k &= 0 \\ V_i - V_{i\,set} &= 0 \\ P_{\text{int}} - P_{scheduled} &= 0 \end{aligned}\right\} \; h(x) = 0$$

$$\left.\begin{aligned} |S_{km}|^2 - |S_{km\,\max}|^2 &\le 0 \\ P_{Gi} - P_{Gi\,\max} &\le 0 \\ P_{Gi\,\min} - P_{Gi} &\le 0 \\ V_i - V_{i\,\max} &\le 0 \\ V_{i\,\min} - V_i &\le 0 \\ t_{km} - t_{km\,\max} &\le 0 \\ t_{km\,\min} - t_{km} &\le 0 \\ \alpha_{km} - \alpha_{km\,\max} &\le 0 \\ \alpha_{km\,\min} - \alpha_{km} &\le 0 \end{aligned}\right\} \; g(x) \le 0$$

It should be noted that the constraints on the reactive power at each generator are not included in the problem as stated above. These constraints will be taken care of by treating a generator bus at a Q limit as a load bus. This is commonly done in a power system when modeling generator reactive power limits [23, p. 228].

2.2.7 Summary of Lagrangian terms

Given the problem statement for the OPF as shown in Section 2.2.5, the Lagrangian can be written as a summation of several terms. These terms are summarized as follows:

$$\left.\begin{array}{rl}
\lambda_{\mathrm{Skm}}\left(\left|\mathrm{S}_{\mathrm{km}}\right|^2-\left|\mathrm{S}_{\mathrm{km}\,max}\right|^2\right) & * \\
\lambda_{\mathrm{Pgih}}\left(\mathrm{P}_{\mathrm{Gi}}-\mathrm{P}_{\mathrm{Gi}\,max}\right) & * \\
\lambda_{\mathrm{PGil}}\left(\mathrm{P}_{\mathrm{Gi}\,min}-\mathrm{P}_{\mathrm{Gi}}\right) & * \\
\lambda_{\mathrm{Vih}}\left(\mathrm{V}_{\mathrm{i}}-\mathrm{V}_{\mathrm{i}\,max}\right) & * \\
\lambda_{\mathrm{Vil}}\left(\mathrm{V}_{\mathrm{i}\,min}-\mathrm{V}_{\mathrm{i}}\right) & * \\
\lambda_{\mathrm{tkmh}}\left(\mathrm{t}_{\mathrm{km}}-\mathrm{t}_{\mathrm{km}\,max}\right) & * \\
\lambda_{\mathrm{tkml}}\left(\mathrm{t}_{\mathrm{km}\,min}-\mathrm{t}_{\mathrm{km}}\right) & * \\
\lambda_{\alpha\mathrm{km}\,max}\left(\alpha_{\mathrm{km}}-\alpha_{\mathrm{km}\,max}\right) & * \\
\lambda_{\alpha\mathrm{km}\,min}\left(\alpha_{\mathrm{km}\,min}-\alpha_{\mathrm{km}}\right) & *
\end{array}\right\}\ \text{inequality constraints}$$

$$\left.\begin{array}{r}
\mu_{\mathrm{Pk}}\left(\mathrm{P}_{\mathrm{k}}\right) \\
\mu_{\mathrm{Qk}}\left(\mathrm{Q}_{\mathrm{k}}\right) \\
\mu_{\mathrm{Viset}}\left(\mathrm{V}_{\mathrm{i}}-\mathrm{V}_{\mathrm{i\,set}}\right) \\
\mu_{int}\left(\mathrm{P}_{int}-\mathrm{P}_{\mathrm{scheduled}}\right)
\end{array}\right\}\ \text{equality constraints}$$

$$\left.\sum_{generators}\left(a_i+b_iP_{Gi}+c_i{P_{Gi}}^2\right)\right\}\ \text{generator cost functions}$$

$$\left.\begin{array}{rl}
k\left(\left|S_{km}\right|^2-\left|S_{km\ \max}\right|^2\right)^2 & * \\
k\left(V_{i\ \min}-V_i\right)^2 & * \\
k\left(V_i-V_{i\ \max}\right)^2 & *
\end{array}\right\}\ \text{penalty functions}$$

Note: The terms with an asterisk (*) next to them are only included when the corresponding constraints are being enforced

2.2.8 Calculation of gradient and Hessian

Given the terms of the Lagrangian, calculation of the gradient and Hessian is a very straightforward process, albeit an extremely tedious one. For completeness, details on calculating the gradient and Hessian are found in Appendices B, C, and D.

2.2.9 Solution of the optimal power flow

Once an understanding of the calculation of the Hessian and gradient is attained, the solution of the OPF can be achieved by using the Newton's method algorithm. The Newton's method algorithm is summarized in the flowchart in Figure 2.1 on page 10. The application of Newton's method to the OPF algorithm used in this thesis is summarized as follows:

Step 1. Initialize the OPF solution.

a. Initial guess at which inequalities are violated.

b. Initial guess z vector (bus voltages and angles, generator output power, transformer tap ratios and phase shifts, all Lagrange multipliers).

Step 2. Evaluate those inequalities that have to be added or removed using the information from Lagrange multipliers for hard constraints and direct evaluation for soft constraints.

Step 3. Determine viability of the OPF solution. Presently this ensures that at least one generator is not at a limit.

Step 4. Calculate the gradient and Hessian of the Lagrangian.

Step 5. Solve the equation $[H]\Delta z = \nabla L(z)$.

Step 6. Update solution $z_{new} = z_{old} - \Delta z$.

Step 7. Check whether $\|\Delta z\| < \varepsilon$. If not, go to Step 4, otherwise continue.

Step 8. Check whether correct inequalities have been enforced. If not go to Step 2. If so, problem is solved.

2.3 A Sample Case Illustrating OPF Algorithm Process

In order to gain insight into the process which the OPF algorithm undergoes while determining the optimum solution, a test was run on a 118-bus system. The details of this system are not included in this thesis because this case is only shown to demonstrate the solution process described in the flowchart of Figure 2.1 on page 10.

The output to a message file during the solution of the 118-bus system is shown in the following.

1. Case OPF Case initialized
2. Starting OPF solution at 15:15:19
3. OPFitr 0 MaxMis: Controls: 25.7240 Voltages: 3113.4475 Angles: 3216.6133 Constraints: 5.8894
4. OPFitr 1 MaxMis: Controls: 0.0000 Voltages: 73.2151 Angles: 29.0626 Constraints: 0.1888
5. OPFitr 2 MaxMis: Controls: 0.0000 Voltages: 0.3480 Angles: 0.1868 Constraints: 0.0067
6. OPFitr 3 MaxMis: Controls: 0.0000 Voltages: 0.0025 Angles: 0.0007 Constraints: 0.0000
7. OPFitr 4 MaxMis: Controls: 0.0000 Voltages: 0.0001 Angles: 0.0002 Constraints: 0.0000
8. Adding Hard MVA Constraint from bus 64 to 65
9. Adding Soft Voltage (high) Constraint at bus 9
10. Adding BusQ Constraint for bus 12
11. Adding Soft Voltage (low) Constraint at bus 53
12. Bus 40 Gen at Max MW Limit
13. OPFitr 5 MaxMis: Controls: 10.0000 Voltages: 571.4009 Angles: 896.2391 Constraints: 1.6602
14. OPFitr 6 MaxMis: Controls: 0.0000 Voltages: 21.5599 Angles: 183.7967 Constraints: 0.3324
15. OPFitr 7 MaxMis: Controls: 0.0000 Voltages: 1.5178 Angles: 19.1469 Constraints: 0.0393
16. OPFitr 8 MaxMis: Controls: 0.0000 Voltages: 0.0233 Angles: 0.3324 Constraints: 0.0009
17. OPFitr 9 MaxMis: Controls: 0.0000 Voltages: 0.0005 Angles: 0.0003 Constraints: 0.0000
18. OPFitr 10 MaxMis: Controls: 0.0000 Voltages: 0.0001 Angles: 0.0004 Constraints: 0.0000
19. OPFitr 11 MaxMis: Controls: 0.0000 Voltages: 0.0001 Angles: 0.0003 Constraints: 0.0000
20. Successful OPF - Final Cost 51324.70 at 15:15:20

This output file can help in the understanding of the Newton's method solution process. Lines 1 and 2 initialize the OPF variables and assume a Lagrangian that contains no constraints. Lines 3 to 7 then perform the inner loop of Newton's method, which continuously solves $[H]\Delta z = \nabla L(z)$ until convergence. After having reached convergence here, the inequality constraints are checked to ensure that none are violated. As can be seen from lines 8 to 12, several inequality constraints are found to be violated: a transmission line has exceeded its MVA capacity, a

generator has exceeded its MVAR limit, a generator has exceeded its MW limit, and two buses are outside their desired ranges. With these violations noted, the Lagrangian is recalculated and the inner loop is begun again. Lines 13 to 19 show the inner loop process proceeding successfully again. After convergence is achieved again, the inequality constraints are again checked. Line 20 shows that new violations were found and the successful final cost is shown.

2.4 Information Gained from the OPF Solution

The solution of the OPF, while difficult, has many great advantages over the classical economic dispatch [11] of a power system. The OPF is capable of performing all of the control functions necessary for the power system. While the economic dispatch of a power system does control generator MW output, the OPF controls transformer tap ratios and phase shift angles as well. The OPF also is able to monitor system security issues including line overloads and low or high voltage problems. If any security problems occur, the OPF will modify its controls to fix them, i.e., remove a transmission line overload.

Besides performing these enhanced engineering functions, probably the greatest advantage of the OPF is the great wealth of knowledge it yields concerning the economics of the power system. In studying the Lagrange multipliers associated with each constraint, one can show that they can be interpreted as the marginal costs associated with meeting the constraint. A derivation of this fact can be found in Appendix A. Therefore, the Lagrange multipliers, μ_{PK} and μ_{QK}, can be seen as the marginal cost of real and reactive power generation at bus k in $\left[\frac{\$}{\text{MW hr}}\right]$ and $\left[\frac{\$}{\text{MVAR hr}}\right]$, respectively. These prices could then be used to determine electricity prices at bus

k. On a larger level, the Lagrange multiplier, μ_{int}, associated with the area interchange constraint, can be seen as the marginal cost of allowing an area to break its interchange. If this cost is positive, then the area would benefit from buying electricity, while if it is negative, the area would benefit from selling electricity. These costs may be of use in determining the price which an area would charge for a megawatt transaction with another area.

While these economic data are very helpful for real-time pricing algorithms, other data could be used to help with transmission system planning. Consider the Lagrange multiplier associated with a hard transmission line MVA constraint, λ_{Skm}. This can be interpreted as the cost savings per hour for each additional 1 MVA increase in a line's rating. This information may be of use in planning where new transmission lines will have the greatest economic impact on the power system.

Much more information can be gained from a single OPF solution, but a great potential also lies in the simulation of a power system over time using a power system simulator with an OPF as its solution engine. This will be discussed in Chapter 4.

3. HEURISTICS OF THE OPTIMAL POWER FLOW SOLUTION

3.1 Classification of OPF Variables

While writing software to perform an OPF solution, a primary concern is identification of variables during the process. Because of this, in order to handle the variables in the OPF problem efficiently, it is convenient to separate them into three categories: controls, states, and constraints. The control variables correspond to quantities that can be arbitrarily manipulated, within their limits, in order to minimize the costs. These include generator MW outputs, transformer tap ratios, and transformer phase shift angles. The states correspond to quantities that are set as a result of the controls, but must be monitored. They are also of interest at the solution. The states include all system voltages and angles. Finally, the constraint variables are variables associated with the constraints. These include all the Lagrange multipliers. The variables in the OPF problem are summarized in Table 3.1.

Table 3.1 OPF problem variables

Variable Classification	Variables in Classification
Control	P_{Gk}, t_{km}, and α_{km}
State	V_k and δ_k
Constraint	μ_{Pk}, μ_{Qk}, μ_{viset}, μ_{int}, λ_{Skm}, λ_{PGih}, λ_{PGil}, λ_{Vih}, λ_{Vil}, $\lambda_{tkm\,max}$, $\lambda_{tkm\,min}$, $\lambda_{\alpha\,km\,max}$, and $\lambda_{\alpha\,km\,min}$

In addition to the OPF variables, it is also important to keep track of any added soft constraints. For hard constraints, the Lagrange multiplier is monitored, but for soft constraints, a fourth

variable classification is added: penalty. No variable data are stored for this classification. It simply serves as a place holder for the penalty function.

3.2 Implementation of Sparse Matrix Techniques

At the heart of the solution of the OPF using Newton's method is the solution of the linear system of equations, $[H]\Delta z = \nabla L(z)$. During the Newton's method solution process, this system of equations is solved repeatedly. Because of this, and because one of the primary objectives of an OPF is to find its solution in a short amount of time, the speed of the solution of this linear system of equations is essential to a successful OPF solution. Fortunately, as is the case with many power system matrices, the Hessian matrix is extremely sparse. By implementing sparse matrix routines, the equations can be quickly solved.

Much of the structure of the Hessian matrix for the OPF problem is known prior to any calculation. In general, for any Newton's method routine, the Hessian takes the following form as discussed in Section 2.1.2:

$$H = \begin{bmatrix} W & J^T \\ J & 0 \end{bmatrix}$$

Already, it is seen that the lower right quadrant of the matrix has entries of zero. By a closer examination of the Hessian structure for the OPF problem, advantage can be taken of this sparsity.

The first step was to reorder the variables to include the generator megawatt controls first, followed by the remaining controls, states, and then constraints. This resulted in the following structure.

$$H = \begin{bmatrix} W_{PG} & 0 & n_{PG}^{T} \\ 0 & W_{remaining} & J_{remaining}^{T} \\ n_{PG} & J_{remaining} & 0 \end{bmatrix}$$

where W_{PG} is a purely diagonal matrix with entries of $2c_i$, n_{PG} is a matrix with a (-1) entry in each column corresponding to the net power injection constraint, and possibly an entry of (±1) in a column corresponding to a generator with a maximum or a minimum MW constraint being enforced, and $W_{remaining}$ and $J_{remaining}$ are the remaining parts of the Hessian matrix.

Due to this structure, the sparse LU factorization up to the rows of $W_{remaining}$, using Gauss's method [24], will result in the following matrix.

$$H_{\text{modified}} = \left[\begin{array}{c|c|c} W_{PG} & 0 & W_{PG}^{-1} n_{PG}^{T} \\ \hline 0 & W_{remaining} & J_{remaining}^{T} \\ \hline n_{PG} & J_{remaining} & -n_{PG} W_{PG}^{-1} n_{PG}^{T} \end{array}\right]$$

$W_{remaining}$ and $J_{remaining}$ are unaffected by these steps and fills are only created by the term $n_{PG} W_{PG}^{-1} n_{PG}^{T}$. In order to determine the fills created by this matrix, consider only its zero/non-zero structure. One will find that most fills created by this term are actually desired.

Because W_{PG} is a diagonal matrix, it will not affect the zero/non-zero structure of the resulting matrix; therefore, only consider the matrix $n_{PG} n_{PG}^{T}$. If no generators are at a megawatt limit, then each column of n_{PG} will have only a single entry of (-1). In this situation, the matrix will result in only diagonal entries in the rows corresponding to the Lagrange multipliers μ_{Pk}. The diagonal entries are needed for factorization anyway, so this is a desired event. If, however, some generators are at a megawatt limit, then the matrix $n_{PG} n_{PG}^{T}$ will have some off-diagonal entries. These entries will occur in off-diagonal pairs such as (row λ_{PGih} ,column μ_{Pk}), and (row μ_{Pk}, column λ_{PGih}) .

Because generators will not be normally at their limits, and because only two non-diagonal fills are created for each generator at a limit, this ordering can help speed the solution. This ordering is what is presently done in the OPF source code written for this thesis.

In studying the Hessian matrix structure further, one can see that the Hessian rows corresponding to the Lagrange multipliers corresponding to the voltage set points contain only one entry, a (+1). In order to exploit this structure, consider ordering the variables in the following manner: generator MW outputs first, voltage states corresponding to generators second, Lagrange multipliers corresponding to generator voltages (in same order as the states) third, and finally the remaining states and constraints. This results in the following structure for the Hessian matrix

$$\mathrm{H} = \begin{bmatrix} W_{PG} & 0 & 0 & 0 & n_{PG}^{T} \\ 0 & W_{vset} & I & W_{rvset}^{T} & J_{rvset}^{T} \\ 0 & I & 0 & 0 & 0 \\ 0 & W_{rvset} & 0 & W_{r} & J_{rr}^{T} \\ n_{PG} & J_{rvset} & 0 & J_{rr} & 0 \end{bmatrix}$$

where I is the identity matrix.

Given this ordering, switching the second- and third-row partitions around yields the following.

$$\mathrm{H} = \left[\begin{array}{ccccc} W_{PG} & 0 & 0 & 0 & n_{PG}^{T} \\ 0 & I & 0 & 0 & 0 \\ 0 & W_{vset} & I & W_{rvset}^{T} & J_{rvset}^{T} \\ \hdashline 0 & W_{rvset} & 0 & W_{r} & J_{rr}^{T} \\ n_{PG} & J_{rvset} & 0 & J_{rr} & 0 \end{array}\right]$$

Given this ordering, the sparse LU factorization up to the rows of W_r, using Gauss's method [24], will result in the following matrix.

$$H_{\text{modified}} = \left[\begin{array}{ccc:cc} W_{PG} & 0 & 0 & 0 & W_{PG}^{-1}\, n_{PG}{}^{T} \\ 0 & I & 0 & 0 & 0 \\ 0 & W_{vset} & I & W_{rvset}{}^{T} & J_{rvset}{}^{T} \\ \hdashline 0 & W_{rvset} & 0 & W_{r} & J_{rr}{}^{T} \\ n_{PG} & J_{rvset} & 0 & J_{rr} & -n_{PG} W_{PG}^{-1}\, n_{PG}{}^{T} \end{array}\right]$$

The fills created by this method would be identical to those created by the previous ordering. However, in addition, the sparse matrix routines could also take advantage of simply "skipping" over the processing of the second- and third-row partitions because the only operations required by Gauss's method would be divisions by 1.

This ordering could be implemented and would result in increased solution speed; however, it does require row pivoting to be done by the sparse matrix solution routines. At present, the implementation of this ability into the OPF source code has not been done, but it can be added at a later time. Presently, the OPF source code does ordering with generator megawatt output controls first.

3.3 Determination of the Set of Binding Inequality Constraints

When reading any paper written about the application of Newton's method to the OPF problem, one runs into discussions of finding the binding set of inequalities [13]. The reason for this emphasis is the role this process has in determining the speed of an OPF solution, and thus ultimately its usefulness. In referring to Figure 2.1 showing the Newton's method solution algorithm, one sees that this determination of the binding set makes up the outer loop of the flowchart. In a typical OPF problem, this outer loop will be executed about three or four times. Therefore, even removing one of these iterations could save 25 - 33% of the execution time assuming that the inner loop time remains relatively constant.

For the OPF source code written for this thesis, the following process was used to determine if the correct inequalities had been enforced.

Step 1. Check if any inequality constraints can be removed. An inequality constraint can be removed if the Lagrange multiplier associated with it is negative.

a. Hard line MVA constraints

b. Hard bus voltage constraints

c. Maximum and minimum generator megawatt outputs

d. Maximum and minimum transformer tap ratios

e. Maximum and minimum transformer phase shifts.

Step 2. Determine if any line MVA limits are violated. If they are, add a hard constraint or soft penalty function depending on user's preference.

Step 3. Determine if any generator reactive power limits are being violated. For those that are violated, change the generator bus to a load bus [23, p. 228].

Step 4. Check if any bus voltage limits are being violated. If they are, add a hard constraint or soft penalty function depending on user's preference.

Step 5. Check all control variables to see if they are operating within their limits. If they are not, add a constraint.

a. Maximum and minimum generator MW outputs

b. Maximum and minimum transformer tap ratios

c. Maximum and minimum transformer phase shifts.

Using this process, the OPF will determine which inequality constraints to enforce.

3.4 Searching Algorithms

While performing the OPF solution, it is often necessary to search through the list of controls, states, and constraints for a particular variable. While for small systems the use of a simple linked list is adequate, when the system becomes large, this searching can begin to dominate the CPU time spent, because with a linked list, the average search time is proportional to half of the number of elements in the list (N/2). It is therefore very useful to take advantage of a data structure suited for repeated searches. One such data structure is the binary tree. A sample binary tree is shown in Figure 3.1.

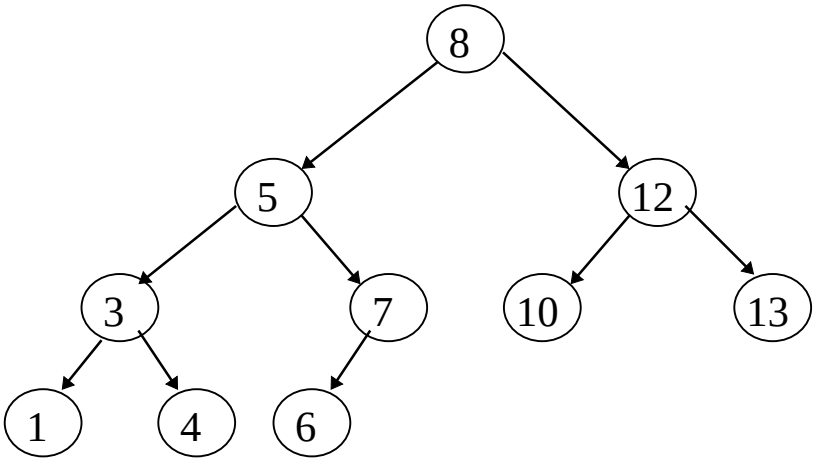

Figure 3.1 Sample Binary Tree

A binary tree obeys very simple rules which make searching for an individual element of the tree a very quick process. At each node, all values to the left of the node are smaller, and all values to the right of the node are larger. In this way, it can be shown that the maximum search time for an element of the tree is proportional to the base two logarithm of the number of elements ($\log_2 N$). The saving in time is substantial when the number of nodes becomes very

large. Consider a system which has 1024 elements: 1024/2 = 512 and $\log_2 1024 = 10$. The binary tree results in an average search which is 50 times faster.

Applying this thinking to OPF variables requires that they be given an ordering so that "smaller than" and "larger than" comparisons can be made. In the OPF source code, the variables are separated, as discussed in Section 3.1, into controls, states, and constraints. For the ranking in this thesis, precedence order is controls, states, and then constraints. Within each variable type precedence is defined as follows:

Controls
1. Bus number (from bus for transformer tap or phase shift)
2. (To bus number for transformer tap or phase shift)
3. Type of control with ranking: P_{Gk}, t_{km}, and α_{km}.

States
1. Bus number
2. Type of state with ranking: V_k and δ_k.

Constraints
1. Bus number (or area number for interchange constraints)
2. (To bus number for line constraints)
3. Type of constraint with ranking: μ_{Pk}, μ_{Qk}, μ_{viset}, μ_{int}, λ_{Skm}, λ_{Pgih}, λ_{PGil}, λ_{Vih}, λ_{Vil}, $\lambda_{tkm\ max}$, $\lambda_{tkm\ min}$, $\lambda_{\alpha\ km\ max}$, and $\lambda_{\alpha\ km\ min}$.

The binary tree structure can then be applied to these structures with this ranking. Using the binary tree data structure greatly aids in reducing the amount of time spent searching.

3.5 Solution of an OPF Repeatedly Over Time

One of the great opportunities of an OPF solution is the ability to simulate a power system over time while keeping it at its optimal solution. This will be discussed in the next section, but heuristics for increasing the computational speed of this process will be discussed here.

As mentioned in Section 2.1, the convergence of Newton's method algorithm is very rapid near the solution. Because of this, the initial guess for the variables is very important. It was also mentioned in the previous section that the speed of the OPF is greatly influenced by how quickly the binding set of inequalities is found. Both of these important parameters for solving the OPF quickly can be met when simulating a power system over time.

By assuming that the power system will not undergo drastic change over the next time step, the output of one OPF solution (the Hessian, gradient, voltages, angles, Lagrange multipliers, as well as which inequalities are binding) can be fed as the initial guess for the next OPF solution. At present, however, the Hessian and gradient of the Lagrangian are recalculated from scratch at each time step of the simulation. The search for the binding inequalities is also done from scratch for each time step. By keeping the solved OPF solution, the speed of solution in the simulation environment will be greatly increased. These modifications will greatly enhance the power system simulation over time.

In calculating the Hessian a time step, further advantage could be gained by implementing partial re-factorization schemes for the Hessian as seen in [25]. These schemes only update those elements of the L and U factors of the Hessian that are affected by changes to the Hessian. While this holds great promise for future work, these schemes have not yet been implemented into the OPF written for this thesis.

4. USES OF AN OPTIMAL POWER FLOW IN A POWER SYSTEM SIMULATION ENVIRONMENT

While a single OPF solution yields valuable information regarding a power system, the implementation of the OPF into a power system simulation environment holds even greater promise. In this environment, simulation of a system over time can be done while maintaining it at its optimal condition. In this way, a vast amount of economic data can be gleaned from the simulation. This chapter will give several examples of the use of the OPF code as implemented into the power system simulator, POWERWORLD [17].

4.1 Example Line Overload Removal

A simple power system not operating under the OPF control is shown in Figure 4.1. For details concerning this power system see Appendix E.

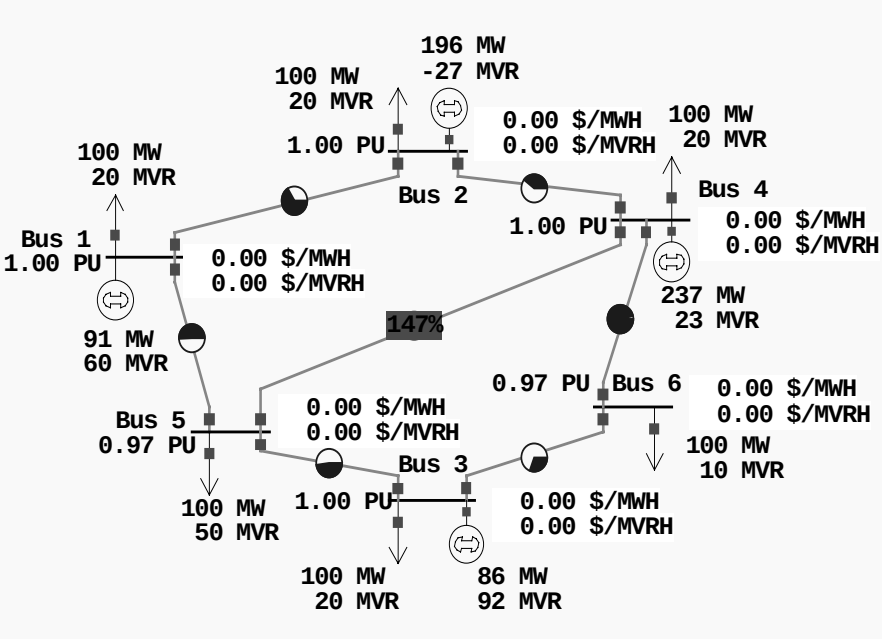

Figure 4.1 Six-bus, Single-Area System Not on OPF Control

In order to remove the line constraint, the OPF control is turned on, and the line overload is removed as shown in Figure 4.2.

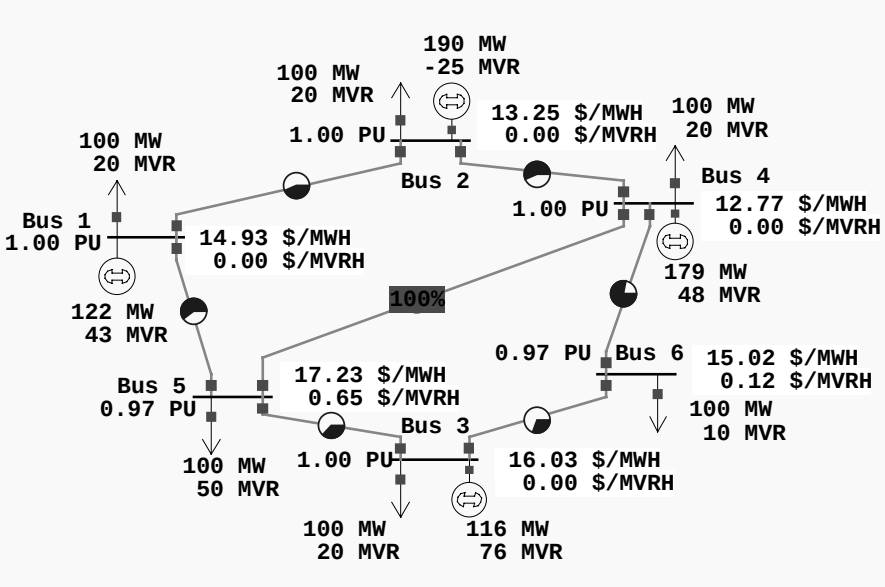

Figure 4.2 Six-bus, Single-Area System on OPF Control

As can be seen, the generators have redispatched themselves in order to remove the line overload. Further analysis of this process from an economic viewpoint will be discussed in the next section.

4.2 Use for Bus Real and Reactive Power Pricing

To illustrate the real and reactive power pricing potentials of the OPF solution, the same system shown in Figure 4.1 is placed on OPF control with its line limit raised. See Figure 4.1. Note that the OPF results in the same dispatch seen in Figure 4.1 now that the line limit has been removed.

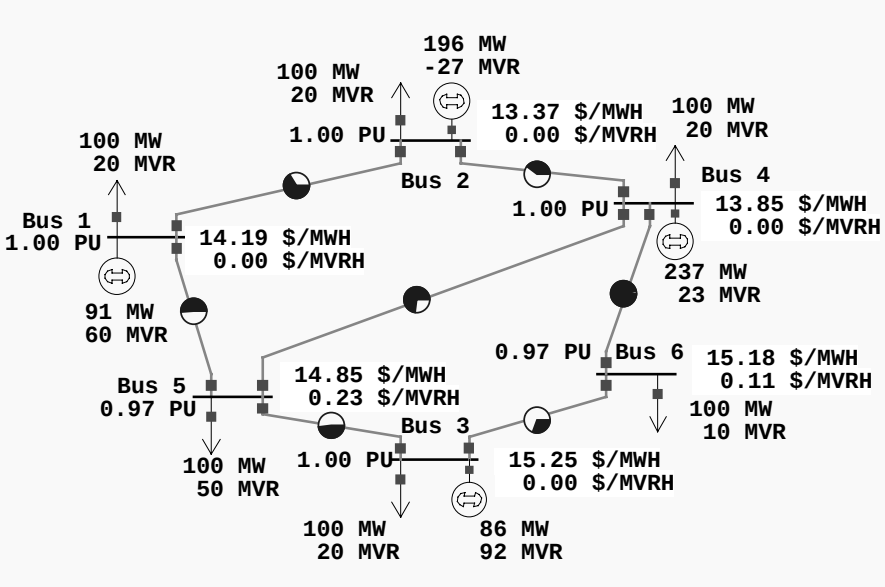

Figure 4.1 Line Limit from Bus 5 to 4 Raised to 100 MVA

Comparison of the OPF solutions in Figure 4.2 and Figure 4.1 yield valuable insight. The total system cost without the line limited as in Figure 4.1 is $7824/hr. With the line limited as in Figure 4.2 this costs increases, as would be expected, to $7895/hr. Also note the differences between the bus MW marginal costs in Figure 4.2 and Figure 4.1. Because the generators at buses 2 and 4 were forced to decrease their output in order to remove the overload, their bus MW marginal costs also decreased. Conversely, the bus MW marginal costs at buses 1, 3, and 5 increased. As might be expected, the largest changes occurred at the ends of the limited line, buses 4 and 5.

4.3 Use for Area Real Power Pricing

The OPF solution method may also be used with multiarea power systems. The OPF will enforce the scheduled area interchange in these systems. In Figure 4.1, the simple six-bus system from before is split into two areas as shown.

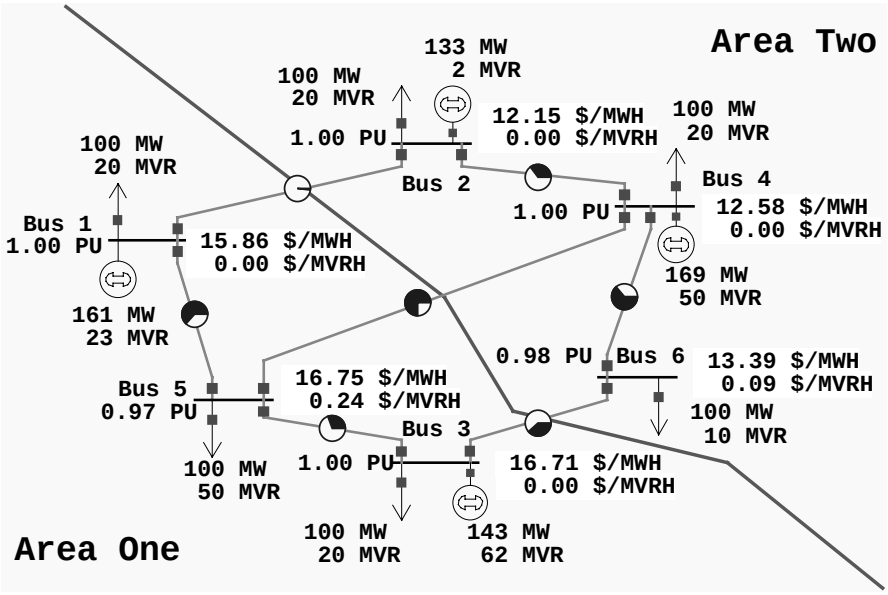

Figure 4.1 Six-bus, Two-Area System on OPF Control

As can be seen, for this case the generation in Area Two is less expensive than in Area One; therefore, it would be advantageous for both areas if Area One were to purchase some power from Area Two. Using the capabilities of the POWERWORLD Area Transactions/Information display [17], scheduled transactions can be set up between the two areas to optimize their costs. Table 4.1 summarizes several possibilities.

Table 4.1 Sample transaction scenarios

Transaction [MW]	Area-One Cost [$/hr]	Area-Two Cost [$/hr]	Sum of Both Areas [$/hr]
None	4564	3496	8060
50.0	4489	3423	7912
65.5	4482	3413	7895
70.0	4481	3415	7896
80.0	4481	3428	7909

As can be seen, the least expensive scenario for the sum of the areas is when an interchange of 65.5 MW is undertaken. This transaction scenario is shown in Figure 4.2.

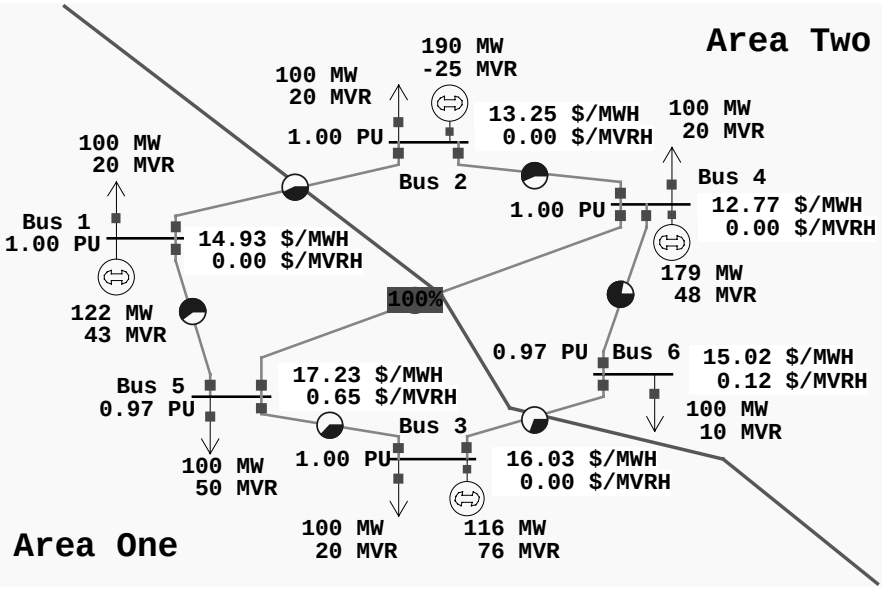

Figure 4.2 Transaction of 65.5 MW Undertaken

Comparing the OPF solution in Figure 4.2 and Figure 4.2 one can see that they show the same solution. This is of course not unexpected, because the two-area economic negotiations should yield the same solution that an OPF solution disregarding areas would. This must happen so that all areas are at their optimal solution.

4.4 Example Transformer Tap Control

In order to test the transformer tap control, a more complex power system was used as in Figure 4.1. This system has 23 buses, 10 generators, 23 transmission lines, and 5 transformers. Three of these transformers are load tap changing (LTC) transformers: buses 5 to 25, 204 to 224, and 102 to 122. For further details, see Appendix F. The system as shown in Figure 4.1 is on OPF control, but the ability to control the tap ratios is turned off and all tap ratios are set at 1 p.u. The system as in Figure 4.2 has activated the tap ratio control functions of the OPF, and the tap ratios have been manipulated so as to minimize the objective function.

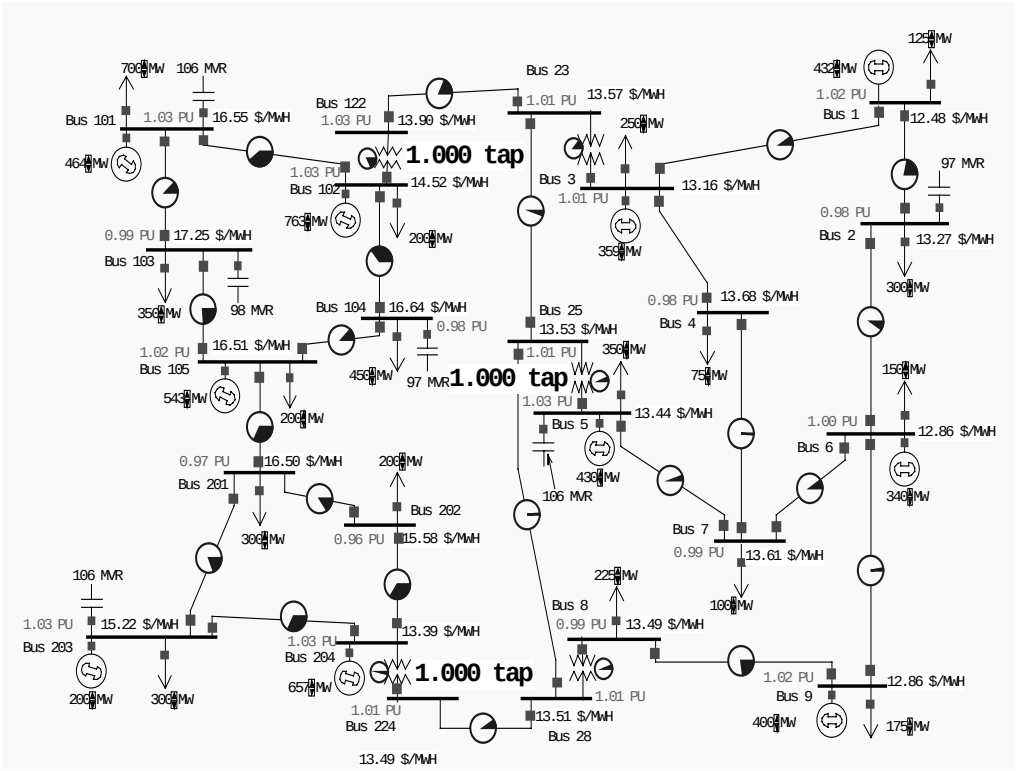

Figure 4.1 Twenty-Three Bus System on OPF Control with Tap Control Off

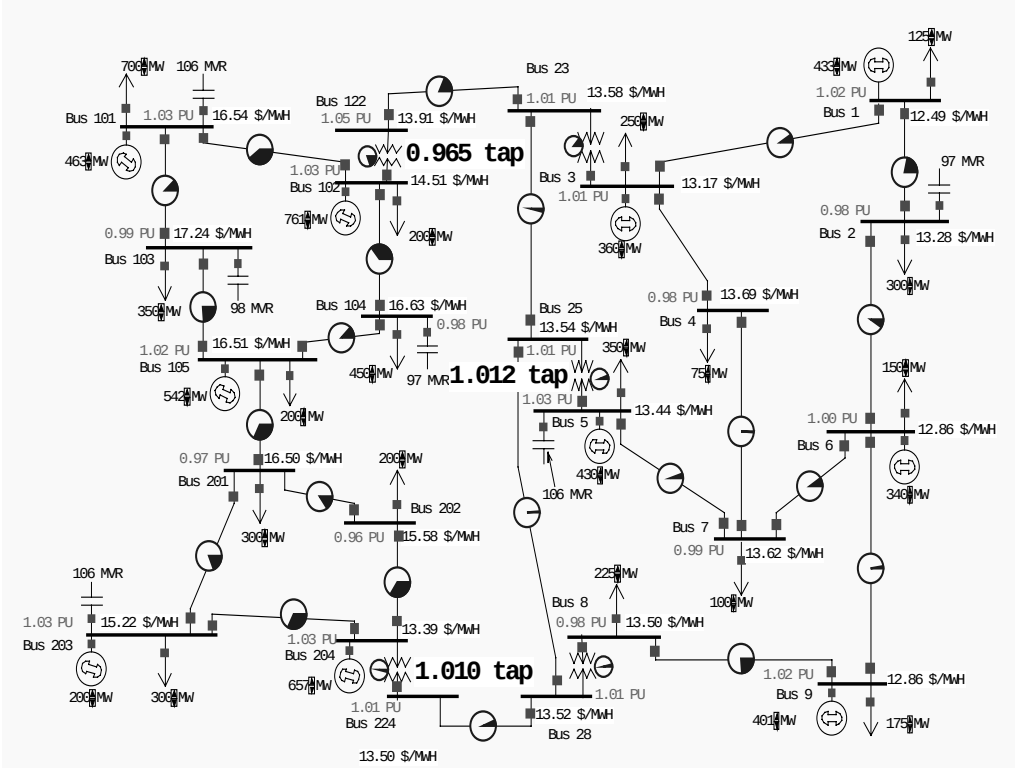

Figure 4.2 Twenty-Three Bus System with Tap Control On

A summary of the tap ratios and resulting total system costs are shown in Table 4.1.

Table 4.1 Summary of tap ratio control experiment

	With tap ratio control OFF	With tap ratio control ON
Tap ratio from bus 5 to 25	1.000 p.u.	1.012 p.u.
Tap ratio from bus 102 to 122	1.000 p.u.	0.965 p.u.
Tap ratio from bus 204 to 224	1.000 p.u.	1.010 p.u.
Total System Cost	$ 50333.25 per hour	$ 50330.55 per hour

As expected, the ability to control tap ratios has lowered the total system cost. It should be noted, however, that the control of the tap ratios will normally not drastically reduce the system costs. In reality, tap ratio control allows control of the reactive power flow thus reducing losses. Even given perfect reactive power control, system losses will only be reduced a small amount; therefore, tap ratio control will not have a huge effect.

4.5 System MVAR Control Using Transformer Taps [26]

As previously mentioned, a tap changing transformer is a reactive power controller. It is this ability which allows it to help control system voltages. Because it controls reactive power, it is also able to reduce system losses by directing the reactive power in a manner which reduces system currents. Because reactive power and real power are not completely decoupled, controlling reactive power can also help with real power control. In this way, a tap changing transformer can help lower generation costs both by reducing system losses and by allowing less expensive generation to operate when it could not have without tap changing control. In this thesis, the OPF has been configured to allow continuous tap values although in reality one encounters discrete tap values (often 33 steps). While modelling the tap as continuous is much easier to implement, it also is better for analyzing the potential abilities of tap changing transformers without the complication of the discrete jumps which would normally occur.

In order to demonstrate a transformer's ability to control the system, consider the seven-bus, one-area system shown in Figure 4.1 (data in Appendix G).

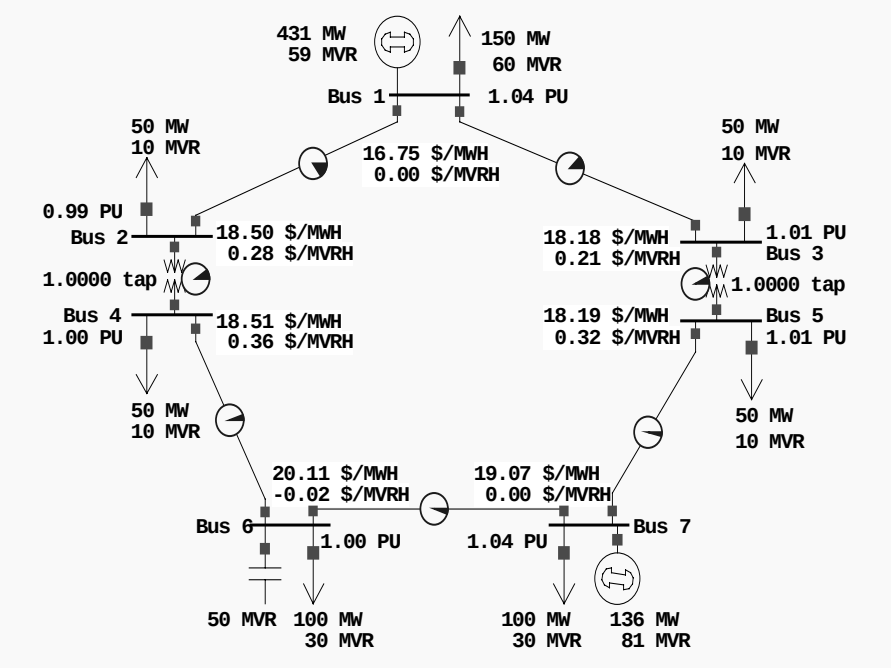

Figure 4.1 Seven-Bus, One-Area System with Taps Inactive

The tap changing ability of the transformers in this system has been deactivated and the OPF solution is shown. This system has a total system cost of $8,059/hr and system losses of 16.22 MW.

Now consider the system with the tap changing abilities activated. The OPF solution is shown in Figure 4.2, and a comparison of the two systems is shown in Table 4.1. Comparing the data in this table, it can be seen that by utilizing the variable tap settings, the system is able to

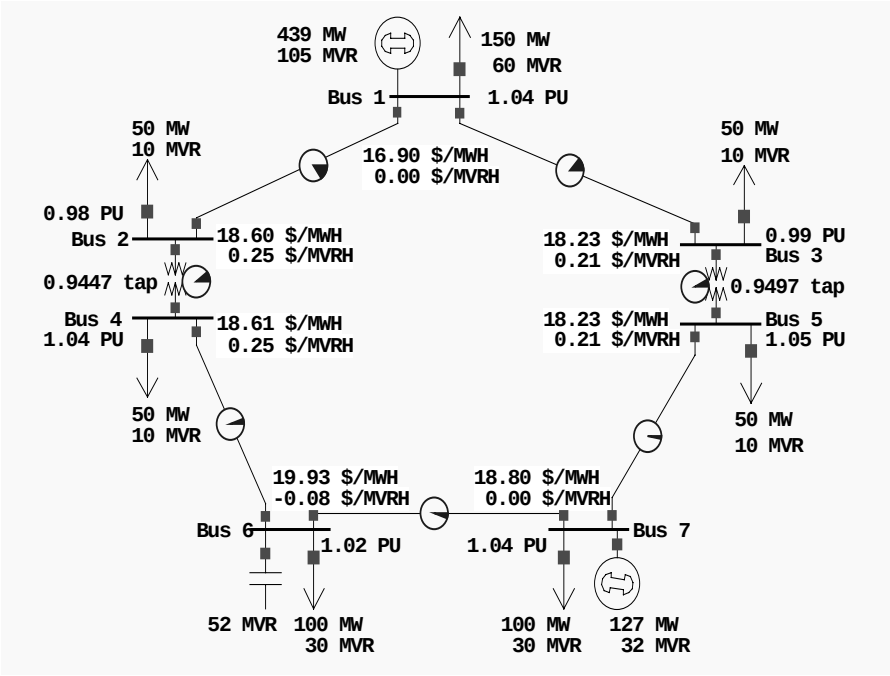

Figure 4.2. Seven-Bus, One-Area, System with Taps Active

Table 4.1 Comparison of two systems

	Without Taps	With Taps
Bus 1 Generation	431 MW 59 MVAR	439 MW 105 MVAR
Bus 7 Generation	136 MW 81 MVAR	127 MW 32 MVAR
System Costs	$8,059/hr	$8,032/hr.
System Losses	16.22 MW	15.73 MW
Tap at bus 2-4	1.000 p.u.	0.9447 p.u.
Tap at bus 3-5	1.000 p.u.	0.9497 p.u.

increase the cheaper generation at bus 1 and ship it towards the bottom of the system while decreasing system losses. This has been done at the expense of greater variability of system voltages. However, all voltages are still within 5% of nominal.

While this example displays the use of the tap changing transformer as a reactive power controller, greater insight can be gained by considering the same system divided into two areas as shown in Figure 4.3. The generation in area one is much less expensive than generation in area two. Therefore it would be beneficial to both parties to undergo a megawatt transaction. Various transactions were undertaken both with the TCUL ability active and with it inactive. Summaries of these results are shown in Table 4.2 and Table 4.3.

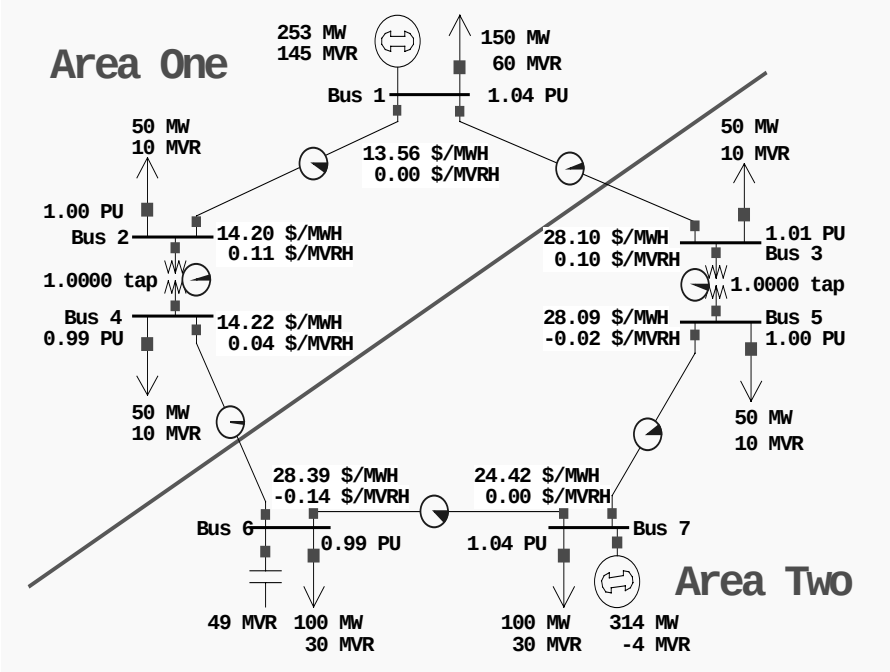

Figure 4.3. Seven-Bus, Two-Area System with Tap-Changing Transformers

Table 4.2 Results for various interchanges with transformer taps left inactive

Interchange Area 1- 2 [MW at $/MWhr]	Bus 1 Gen [MW]	Bus 1 Gen [MVAR]	Bus 7 Gen. [MW]	Bus 1 Gen [MVAR]	Tap Bus 2-4 [p.u.]	Tap Bus 3-5 [p.u.]	Cost at Area 1 [$/hr]	Cost at Area 2 [$/hr]	Total Cost [$/hr]	Losses Area 1 [MW]	Losses Area 2 [MW]	Total Losses [MW]
none	253	145	314	-4	1.0000	1.0000	2,949	6,308	9,257	3.45	14.16	17.61
+50 at 18.84	304	114	258	17	1.0000	1.0000	2,718	5,923	8,641	4.19	7.88	12.07
+50 at 18.46	357	88	204	42	1.0000	1.0000	2,582	5,667	8,249	6.80	4.14	10.94
+50 at 18.12	411	66	153	71	1.0000	1.0000	2,543	5,529	8,072	11.27	2.84	14.11
+19 at 17.84	432	58	134	82	1.0000	1.0000	2,555	5,504	8,059	13.46	2.98	16.44
+31 at 17.84	468	48	104	103	1.0000	1.0000	2,603	5,500	8,103	17.60	3.96	21.56
+50 at 17.37	526	34	58	139	1.0000	1.0000	2,779	5,559	8,338	25.83	7.51	33.34

Table 4.3 Results for various interchanges with transformer taps active

Interchange Area 1- 2 [MW at $/MWhr]	Bus 1 Gen [MW]	Bus 1 Gen [MVAR]	Bus 7 Gen. [MW]	Bus 1 Gen [MVAR]	Tap Bus 2-4 [p.u.]	Tap Bus 3-5 [p.u.]	Cost at Area 1 [$/hr]	Cost at Area 2 [$/hr]	Total Cost [$/hr]	Losses Area 1 [MW]	Losses Area 2 [MW]	Total Losses [MW]
none	253	104	314	36	1.0432	1.0466	2,938	6,299	9,237	2.60	13.79	16.39
+50 at 18.83	304	98	258	34	1.0137	1.0209	2,716	5,921	8,637	4.01	7.84	11.85
+50 at 18.45	357	97	204	32	0.9851	0.9933	2,584	5,664	8,248	6.86	4.04	10.90
+50 at 18.12	411	101	152	32	0.9578	0.9645	2,542	5,514	8,056	11.15	2.14	13.29
+25 at 17.83	439	105	127	32	0.9448	0.9499	2,557	5,475	8,032	13.84	1.86	15.70
+25 at 17.83	467	105	102	38	0.9340	0.9411	2,593	5,462	8,055	16.91	1.99	18.90
+50 at 17.31	524	99	54	60	0.9265	0.9280	2,754	5,491	8,245	24.19	3.73	27.92

A comparison of Table 4.2 and Table 4.3 shows reduced costs at every step for the system with the tap changing transformer active. From a total system cost point of view, the two areas should stop undergoing transactions after having reached the transactions shown in bold type (minimum total cost). This is after a transaction of 169 MW for the system with taps inactive, and a transaction of 175 MW for the system with taps active. Note that after undergoing these transactions, the systems are at the same state found by running the OPF with no area constraints enforced.

The information in these tables illustrates the concept that the tap changing transformer is a reactive power controller. With taps inactive as in Table 4.2, the only elements of the system that have control over the reactive power flows are the two generators. As a result, the variation in the injected reactive power from the generators is extremely large. With the taps active as in Table 4.3, the transformers take over as the reactive power controllers, and as a result, the generators' reactive power injections are able to remain relatively constant.

It should be noted that if a generator were to be treated as an MVA limited machine, as opposed to an MW and MVAR (separately) limited machine, then this reactive power control by the tap changing transformers would free up the generator for more megawatt production.

4.6 Transmission Line Valuation by Time-Domain Simulation

One of the most intriguing potential uses of an OPF is its use as a pricing tool by doing time-domain simulations of a power system. As a simple example, consider again the six-bus, one-area power system of Appendix E again. Assume that the loads of the system vary as shown in

Figure 4.1. The load at a given bus is then equal to its base value shown in Appendix D multiplied by the load factor.

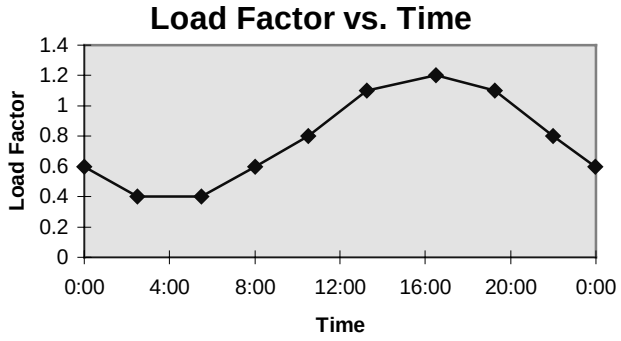

Time	Load Factor	Time	Load Factor
0:00	0.6	13:15	1.1
2:30	0.4	16:30	1.2
5:30	0.4	19:15	1.1
8:00	0.6	22:00	0.8
10:30	0.8	23:59	0.6

Figure 4.1 Load Factor Curve for six-bus System

Entering this load factor curve into the POWERWORLD simulation software and simulating the power system for a full 24 hours yield a total cost in dollars for operating the power system over that period of time. By re-simulating the system repeatedly with variations in system structure, one can gain useful economic insights from the comparison of total system costs. Note that the case was simulated at 600 times real time for the first 23 hours and at 60 times real time for the last hour. The POWERWORLD simulation software utilizes trapezoidal rule integration to calculate the total system cost from the incremental costs at each time point.

Using this technique, the six-bus system was simulated with various transmission lines removed. The results are summarized in Table 4.1.

Table 4.1 Simulation data for six-bus system with transmission lines removed

System Configuration	Total Cost for 24 Hour Simulation	Difference from No Change Configuration	Percent Increase from No Change Configuration
No Changes	$ 148,240	N/A	N/A
Line from Bus 3 to Bus 5 Removed	$ 148,377	$137.00	0.09%
Line from Bus 3 to Bus 4 Removed	$ 148,632	$392.00	0.26%
Line from Bus 1 to Bus 2 Removed	$ 149,311	$1,071.00	0.72%
Line from Bus 4 to Bus 5 Removed	$ 150,309	$2,069.00	1.40%

By comparing the total system cost with all lines connected to the cost with a line removed, one can find the approximate cost a company would incur per day while taking a line out for maintenance. It is very important to note, however, that this does in no way take into account the possibility that another line may unexpectedly go out, in which case all lines may be needed to take up the slack. In other words, the pricing of redundancies in the transmission system is not considered in this methodology. Regardless of this, the information is very valuable and could be used to help with maintenance scheduling, or even possibly in helping to determine where to build new transmission lines in the future.

4.7 Capacitor Bank Valuation by Time-Domain Simulation

The technique discussed in Section 4.5 can also be applied to the valuation of any transmission system component. As an example, consider capacitor bank valuation for the twenty-three bus, one-area power system of Appendix E. Assume that the loads of the system vary as shown in Figure 4.1.

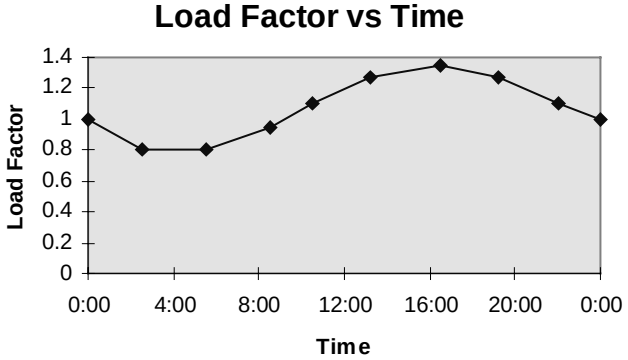

Time	Load Factor	Time	Load Factor
0:00	1.000	13:15	1.275
2:30	0.800	16:30	1.350
5:30	0.800	19:15	1.275
8:30	0.950	22:00	1.100
10:30	1.100	23:59	1.000

Figure 4.1 Load Factor Curve for Twenty-Three Bus System

Again, entering this load factor curve into the POWERWORLD simulation software and simulating the power system for a full 24 hours yield a total cost in dollars for operating the power system over that period of time. Following the technique as shown before, the twenty-three bus system was simulated with various capacitor banks removed. The results are summarized in Table 4.1. This simulation was run at 60 times real time for the entire simulation.

Table 4.1 Simulation data for six-bus system with transmission lines removed

System Configuration	Total Cost for 24 Hour Simulation	Difference from No Change Configuration	Percent Increase from No Change Configuration
No Changes	$ 1,358,423	N/A	N/A
Capacitor Bank at bus 103 Removed	$ 1,359,609	$1,186.00	0.0873%
Capacitor Bank at bus 2 Removed	$ 1,359,222	$799.00	0.0588%
Capacitor Bank at bus 104 Removed	$ 1,359,626	$1,203.00	0.0886%

Again, from this information, the approximate cost a company would incur per day while removing the capacitor bank can be inferred from these calculations.

4.8 Limit on Available Transfer Capability (ATC) Due to a Voltage Constraint [26]

Another use for the OPF algorithm is for the calculation of the available transfer capability for a system. The OPF is able to take into account system security concerns including voltage limits and transmission line limits while calculating the ATC.

The three-bus system of Figure 4.1 (data in Appendix H) can be used to illustrate and examine the value of reactive power support at a system load bus. Area one consists only of the generator and load at bus 1 plus two tie lines. Area two consists of the generator and load at bus 3 plus the load at bus 2, and the line from bus 2 to bus 3. Area one has expensive generation,

while area two has cheaper generation. For the indicated loads and no area transfers the cost of operation for the total system is $25,799/hr. For this study, the loads at all buses remain fixed at the values shown.

The base case shown in Figure 4.1 has each area providing its own load plus a portion of the system losses. The unfilled pie charts on each line indicate that the lines are loaded at less than their MVA ratings. This base case has zero scheduled megawatt transfer between the two areas, but 73 MW of area two's generation flows through area one.

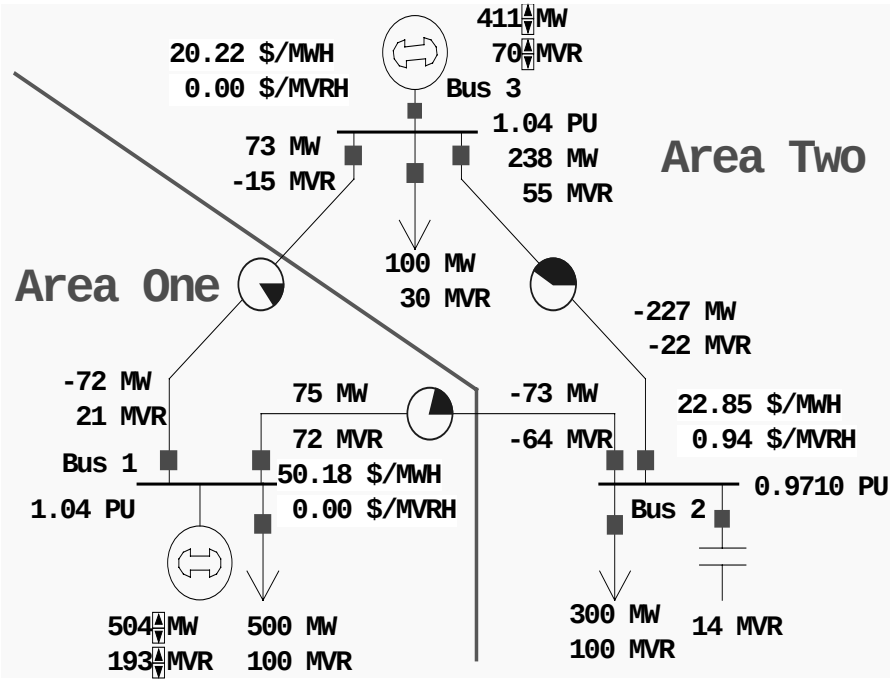

Figure 4.1 Three-Bus Base Case with No Area Power Transfer

Note that the incremental cost for reactive power at a generator bus is $0.00. This is true as long as no MVAR limits are reached because no cost is associated with generation of MVARs by a generator in the OPF formulation of this thesis.

Consider the situation where area one wants to purchase power at considerable savings from area two. Similarly, area two wants to sell power to area one. We first examine the available

transfer capability of this system for transfer from area two to area one. An OPF solution with bus voltage constraints is used to find the maximum power which can be transferred from area two to area one. The voltage constraint for power quality used in this example is

$$0.96 \leq V_i \leq 1.04.$$

Both generators have their excitations set to give 1.04 p.u. voltage for serving their local area load within the voltage constraints. A global OPF solution which minimizes the total cost of providing the total load will attempt to increase area-two generation and decrease area-one generation. This power transfer will change the voltage at bus 2. When the transfer is such that the voltage reaches its lower limit (0.96), the OPF solution will stop at that constraint. The solution and associated marginal costs for both real and reactive power at each bus are shown in Figure 4.2 for the case in which a nominal 15 MVAR capacitor bank is installed at bus 2 for reactive power support. The available transfer capability for these constraints is 244 MW. The cost of operation for the total system is $21,341/hr. Thus this maximum power transfer has resulted in a reduction of total cost by $4,458/hr. Additional transfers are not possible without violation of the voltage constraint at bus 2. Note that the incremental cost for MVARs is almost the same as for MWs at bus 2.

When the capacitor bank at bus 2 is increased from a nominal 15 MVAR rating to a nominal 30 MVAR rating, the OPF solution is given in Figure 4.3. The available transfer capability for these constraints is increased to

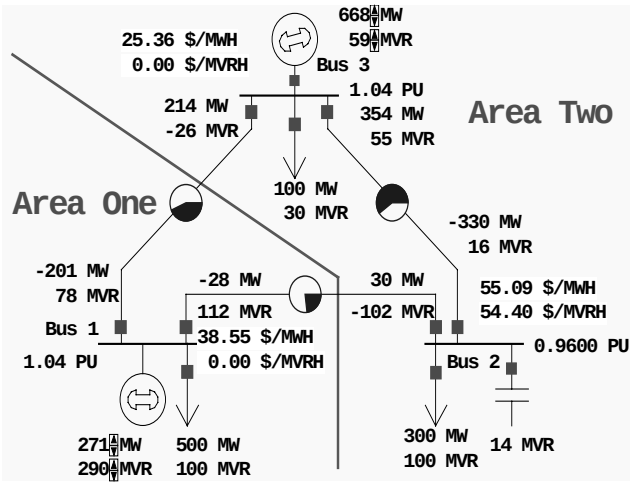

Figure 4.2 Three-Bus Example at Maximum Power Transfer (15 MVAR Capacitor Support)

325 MW. The cost of operation for the total system is $20,890/hr. Thus the increase in available power transfer capability has resulted in an additional reduction of total cost by $451/hr. Again, additional transfers are not possible without violation of the voltage constraint at bus 2. Note that the incremental cost for MVARs has reduced as the OPF approaches a more economical dispatch.

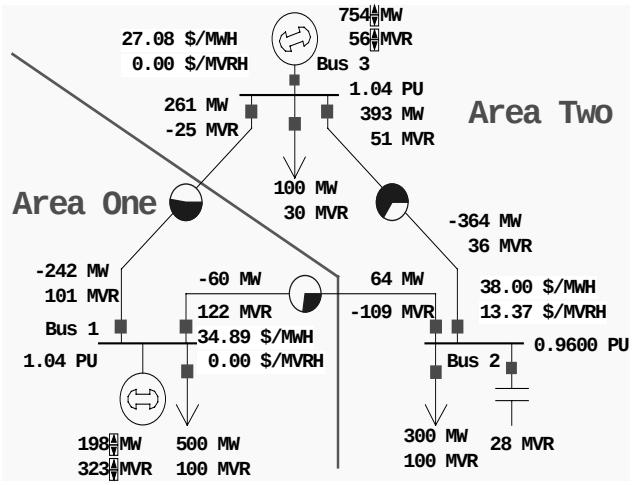

Figure 4.3 Three-Bus Example at Maximum Power Transfer (30 MVAR Capacitor

When the capacitor bank at bus 2 is increased from a nominal 30 MVAR rating to a nominal 45 MVAR rating, the OPF solution is given in Figure 4.4. The available transfer capability for these constraints is increased to 355 MW. The cost of operation for the total system is $20,849/hr. Thus the increase in available power transfer capability has resulted in a further reduction of total cost by $41/hr. Note that the OPF has reached an optimal dispatch schedule without hitting the bus 2 voltage constraint (0.963 > 0.96). Therefore, no additional power transfers can lower the total system costs.

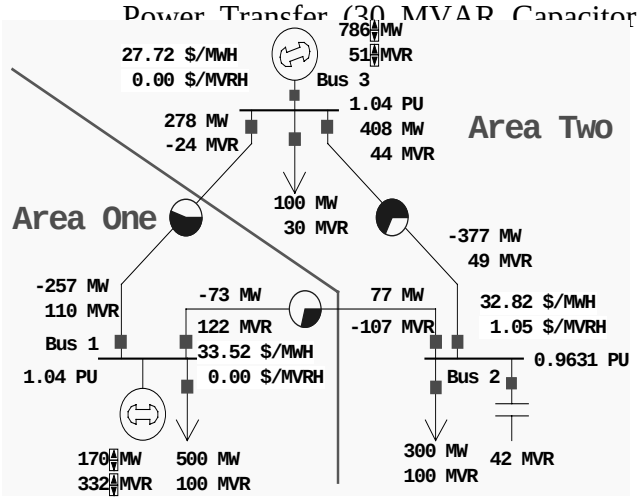

Figure 4.4 Three-Bus Example at Maximum Power Transfer (45 MVAR Capacitor Support)

The savings between 15 and 30 MVAR capacitors was $451 while the savings between 30 and 45 MVAR capacitors was only $41, because there is a greater change in system megawatt

dispatch when moving from 15 to 30 MVAR than from 30 to 45 MVAR. This is also reflected in the incremental costs of MVAR at bus 2 for the various cases.

4.9 Transmission System Pricing Through Short-Run Marginal Costing (SRMC)

In the restructured environment of the future, it may be necessary to determine the cost incurred to the transmission system due to a power transaction between two companies. This cost would be charged to the two companies undergoing the transaction and would be paid to the operator of the transmission system. Two methods proposed for the determination of this cost is through short-run marginal costing (SRMC) and long-run marginal costing (LRMC). These two topics are extensively discussed in both [27] and [28]. A brief, albeit simple, explanation of these follows.

The SRMC takes into account only the operating costs of the power system. The operating costs include fuel costs, losses, as well as system constraints such as transmission line limits. The LRMC, however, includes both the operating costs and the capital costs of the power system. The capital costs include the costs of future expansion to the transmission system as well as the generation capacity.

Through the use of the OPF, the SRMC technique can easily be implemented as discussed in [28]. The SRMC of a power transaction can be estimated by solving the OPF for both the system with the transaction and the system without the transaction in place. After these solutions are obtained, the SRMC can be found as follows.

Define BMC_i = (marginal cost of power at bus i after the transaction)
$P_{i,transaction}$ = the net power injection at bus i due to the transaction
= (- power generation at bus i before transaction
+ power generation at bus i after transaction)

From these definitions a definition for SRMC can then be made [28].

$$SRMC_{transaction} = \sum_{\substack{\text{all buses} \\ \text{in transaction}}} \text{BMC}_i * P_{i,transaction}$$

As a simple example consider the six-bus, two-area system from Section 4.3. Figure 4.1 on page 36 shows this system with no transactions, and Figure 4.2 on page 37 shows the system with a transaction of 65.5 MW undertaken between the two areas. Taking the data from these two figures, a calculation of the SRMC for the transaction can be made. This calculation is summarized in Table 4.1.

Table 4.1 SRMC calculation for six-bus, two-area system

Bus Num	Generation Before Transaction [MW]	BMC Before Transaction [$/MWhr]	Generation After Transaction [MW]	BMC After Transaction [$/MWhr]	$P_{i,trans}$ [MW]	$BMC_i * P_{i,trans}$ [$/hr]
1	161	15.86	122	14.93	-39	-582.27
2	133	12.15	190	13.25	57	755.25
3	143	16.71	116	16.03	-27	-432.81
4	169	12.58	179	12.77	10	127.70
				$SRMC_{transaction} = \sum_{\text{all buses in transaction}} \text{BMC}_i * P_{i,transaction} =$		-132.13

Thus, the SRMC for this transaction is (- $132.13)/hour. As mentioned in [27], SRMC can be a negative value.

For comparison, consider the same system undergoing the same 65.5 MW transaction, but with the line between buses 4 and 5 doubled to 100 MVA from 50 MVA. The simulation of this system is shown in Figure 4.1.

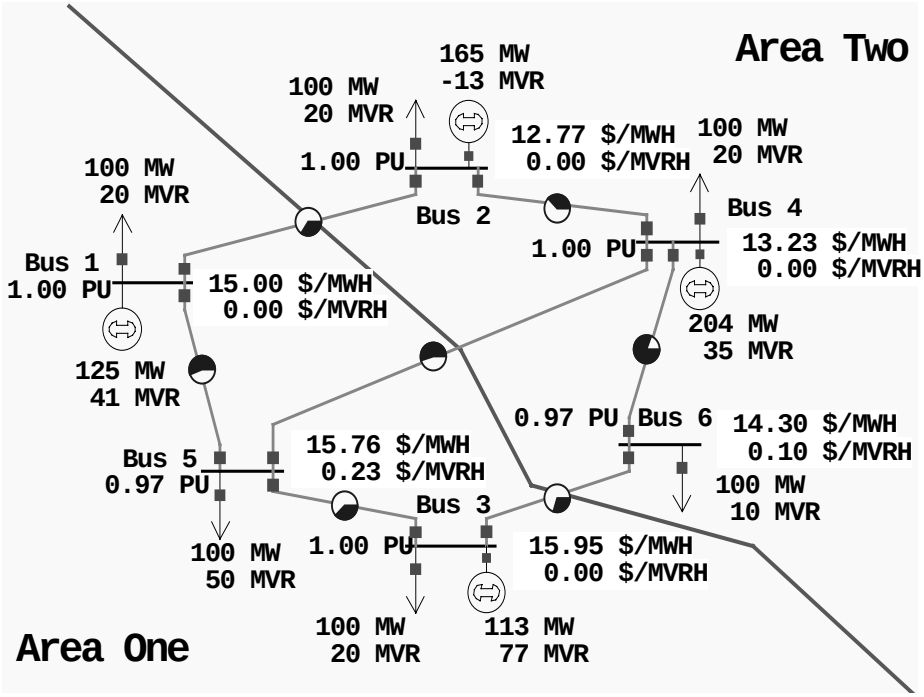

Figure 4.1 Six-bus, Two-Area System Undergoing Transaction with Line Limit Doubled

Again, Figure 4.1 shows this system with no transactions, and Figure 4.2 shows the system with a transaction of 65.5 MW undertaken between the two areas. Taking the data from these two figures, a calculation of the SRMC for the transaction can be made for the system where no line limit will be encountered. This calculation is summarized in Table 4.2.

Table 4.2 SRMC calculation for six-bus, two-area system where no limit is encountered

Bus Num	Generation Before Transaction [MW]	BMC Before Transaction [$/MWhr]	Generation Aafter Transaction [MW]	BMC After Transaction [$/MWhr]	$P_{i,trans}$ [MW]	$BMC_i * P_{i,trans}$ [$/hr]
1	161	15.86	125	15.00	-36	-540.00
2	133	12.15	165	12.77	32	408.64
3	143	16.71	113	15.95	-30	-478.50
4	169	12.58	204	13.23	35	463.05
				$SRMC_{transaction} = \sum_{\text{all buses in transaction}} BMC_i * P_{i,transaction} =$		-146.81

Thus, the SRMC for this transaction is (- $146.81)/hour. This is not unexpected. The previous system encountered a transmission line constraint, while this one has not; therefore, the incentive to do the transaction should be large, i.e., the SRMC should be less.

While this discussion is not entirely complete, it does display the basic use of the OPF to calculate the SRMC. More study will be done on this topic in the future.

5. CONCLUSION

The OFP written for this thesis has been very successful in achieving the goals set forth for an OPF. Minimization of system costs, while maintaining system security, was accomplished through the implementation of Newton's method to the OPF problem. Newton's method has proven to be very adept at solving the OPF problem.

Many applications of the OPF have also been shown as in Chapter 4. The OPF performs generator control and transmission system control while taking into account system limits. The marginal cost data from the OPF were shown to aid in the available transfer capability (ATC) calculation, real and reactive power pricing, transmission system pricing, and transmission system component valuation.

At present, the OPF works very well for small systems (less than 200 buses). Improvements will need to be made to this in order for the software to be truly useful. This can and will be done with relatively minor modifications. As discussed in Section 3.5, by keeping the previous OPF solution from time step to time step, the speed of the OPF solution will be increased. This will allow larger systems to be simulated. The author also plans to implement the partial re-factorization schemes for the Hessian as seen in [25]. These improvements to the software will allow the simulation of systems with thousands of buses. With this ability, the use of the OPF in a power system simulation environment will be truly useful.

Another problem which should be addressed is the modeling of discrete variables within the OPF framework. At present, variables such as transformer tap ratios and phase shift angles are treated as continuous variables.

As a final note for this thesis, the author would like to reiterate that while the applications of the OPF as discussed in this thesis are extremely valuable, they do not take into account the possibility of random outages of transmission line components or generators. Also, the pricing schemes discussed do not take into account the need for future expansion of the power system.

APPENDIX A. ECONOMIC INTERPRETATION OF THE LAGRANGE MULTIPLIERS

The Lagrange multipliers found in the optimal solution can be given an economic interpretation. One can show that the Lagrange multipliers are the negative of the derivative of the function which is being minimized with respect to the enforced constraint. In other words, they are the marginal costs associated with enforcing the constraint. A proof of this as taken from [29] follows.

The non-linear programming problem that is being solved can be expressed in the following form (excluding inequality constraints).

Minimize $f(x)$ (the objective function)

subject to: $h_i(x) = u_i, \quad i = 1, 2, \ldots, m$ (equality constraints)

Therefore, the Lagrange function may be written:

$$L(x(u),\lambda(u),u) = f(x(u)) + \lambda^T(u)\left[h(x(u)) - u\right]$$

with $\lambda(u)$ is a vector of Lagrange multipliers

The optimal solution for u = 0 is (x^*, λ^*). In this problem formulation, the values of u_i are constraints on some resource. One can see that if this constraint value were varied, the optimal solution (x^*, λ^*) would change. The sensitivity to a change in u is desired. This sensitivity can be expressed as the derivative of the Lagrange function with respect to the variable u. Evaluating this derivative yields

$$\nabla_u L(x,\lambda,u) = \frac{\partial x}{\partial u}\nabla_x f(x(u)) + \frac{\partial x}{\partial u}\frac{\partial h(x(u))}{\partial x}\lambda(u) + \frac{\partial \lambda(u)}{\partial u}\left[h(x(u)) - u\right] - \lambda(u)$$

Grouping terms of this functions gives

$$\nabla_u L(x,\lambda,u) = \underbrace{\frac{\partial x}{\partial u}\left[\nabla_x f(x(u)) + \frac{\partial h(x(u))}{\partial x}\lambda(u)\right]}_{\text{First Term}} + \underbrace{\frac{\partial \lambda(u)}{\partial u}\left[h(x(u)) - u\right]}_{\text{Second Term}} - \lambda(u)$$

Now, study the first two terms of this more closely.

$$\left[\nabla_x f(x(u)) + \frac{\partial h(x(u))}{\partial x}\lambda(u)\right] = \nabla_x L(x,\lambda,u)$$

$$\left[h(x(u)) - u\right] = \nabla_\lambda L(x,\lambda,u)$$

Thus the following is written

$$\nabla_u L(x,\lambda,u) = \underbrace{\frac{\partial x}{\partial u}\nabla_x L(x,\lambda,u)}_{\text{First Term}} + \underbrace{\frac{\partial \lambda(u)}{\partial u}\nabla_\lambda L(x,\lambda,u)}_{\text{Second Term}} - \lambda(u)$$

By the Kuhn-Tucker optimality conditions [20, p. 284], both $\nabla_x L(x,\lambda,u)$ and $\nabla_\lambda L(x,\lambda,u)$ must be zero at the optimal solution. Therefore, both the first and second terms must be zero at the optimal solution, and the following is left at the optimal solution

$$\nabla_u L(x^*,\lambda^*) = -\lambda^*$$

We also know that at the optimal solution,

$$\nabla_u L(x^*,\lambda^*) = \nabla_u f(x^*)$$

Combining these two equations, it is seen that at the optimal solution, the following is true.

$$\lambda^* = -\nabla_u f(x^*)$$

Thus the Lagrange multipliers are the negatives of the derivative of the function which is being minimized with respect to the enforced constraint. If the objective function is considered a cost function, then the λ^* can be interpreted as the cost per unit of the resources associated with each constraint. These Lagrange multipliers are thus often referred to as the shadow prices.

Although the previous derivation has not included inequality constraints, the derivation with them included is essentially the same. A simple explanation will be proved here. For all inequality constraints not being enforced (i.e., they are not active), the derivative of the objective function with respect to them will be zero, because the problem solution will not be affected by changing the constraint (u_i) since it is not being enforced anyway. As for the inequality constraints that are being enforced, they will simply behave like equality constraints and the previous derivation can be applied to them.

APPENDIX B. CALCULATION OF THE GRADIENT OF THE LAGRANGIAN

Appendix B contains a list of all the terms that make up the gradient of the Lagrangian for the OPF. The listing is organized by those equations or constraints which result in the addition of the gradient term.

Note: The terms that are shown surrounded by parenthesis, (), are not always part of the gradient. They are dependent on the inequality constraints being enforced.

Note: Many terms are surrounded by brackets, []. Appendix D contains a further explanation of the calculation of these terms.

Gradient term due to generator cost curves (the objective function)

$$\frac{\partial L}{\partial P_{Gi}} = b_i + 2c_i P_{Gi}$$

Gradient terms due to the power flow equations

$$\frac{\partial L}{\partial V_i} = \sum_k \left\{ \mu_{Pk} \left[\frac{\partial P_k}{\partial V_i} \right] + \mu_{Qk} \left[\frac{\partial Q_k}{\partial V_i} \right] \right\} \qquad \frac{\partial L}{\partial \delta_i} = \sum_k \left\{ \mu_{Pk} \left[\frac{\partial P_k}{\partial \delta_i} \right] + \mu_{Qk} \left[\frac{\partial Q_k}{\partial \delta_i} \right] \right\}$$

$$\frac{\partial L}{\partial \mu_{Pk}} = P_k \qquad \frac{\partial L}{\partial \mu_{Qk}} = Q_k \qquad \frac{\partial L}{\partial P_{Gi}} = -\mu_{Pk}$$

Gradient terms due to generator voltage set points

$$\frac{\partial L}{\partial V_i} = \mu_{viset} \qquad \frac{\partial L}{\partial \mu_{viset}} = V_i - V_{Gi\,set}$$

Gradient terms due to maximum and minimum generator power output

$$\frac{\partial L}{\partial \lambda_{PGil}} = \left(-P_{Gi} + P_{Gi\min}\right) \qquad \frac{\partial L}{\partial \lambda_{PGih}} = \left(+P_{Gi} - P_{Gi\max}\right)$$

$$\frac{\partial L}{\partial P_{Gi}} = \left(-\lambda_{PGil}\right) + \left(\lambda_{PGih}\right)$$

Gradient terms due to enforcement of hard transmission line constraints

$$\frac{\partial L}{\partial \lambda_{Skm}} = \left(\left|S_{km}\right|^2 - \left|S_{km\max}\right|^2\right) \qquad \frac{\partial L}{\partial x} = \left(\lambda_{Skm}\left[\frac{\partial \left|S_{km}\right|^2}{\partial x}\right]\right)$$

where $x = V_k, V_m, \delta_k$, or δ_m

Gradient terms due to enforcement of soft transmission line constraints

$$\frac{\partial L}{\partial x} = \left(2k\left(\left|S_{km}\right|^2 - \left|S_{km\max}\right|^2\right)\left[\frac{\partial \left|S_{km}\right|^2}{\partial x}\right]\right) \quad \text{where } x = V_k, V_m, \delta_k, \text{ or } \delta_m$$

Gradient terms due to enforcement of area interchange constraints

$$\frac{\partial L}{\partial \mu_{\text{int}}} = \sum_{\text{tie lines}}\{P_{km}\} - P_{sched} \qquad \frac{\partial L}{\partial x} = \mu_{\text{int}} \sum_{\text{tie lines}}\left[\frac{\partial P_{km}}{\partial x}\right]$$

where $x = V_k, V_m, \delta_k$, or δ_m

Gradient terms due to enforcement of hard voltage constraints

$$\frac{\partial L}{\partial V_i} = \left(\lambda_{vih}\right) + \left(-\lambda_{vil}\right) \qquad \frac{\partial L}{\partial \lambda_{vil}} = \left(-V_i + V_{i\min}\right)$$

$$\frac{\partial L}{\partial \lambda_{vih}} = \left(+V_i - V_{i\max}\right)$$

Gradient terms due to enforcement of soft voltage constraints

$$\frac{\partial L}{\partial V_i} = \left(-2k\left(-V_i + V_{i\min}\right)\right) \qquad \frac{\partial L}{\partial V_i} = \left(+2k\left(V_i - V_{i\max}\right)\right)$$

Gradient terms due to tap changing transformers

$$\frac{\partial L}{\partial \lambda_{tkm\max}} = \left(t_{km} - t_{km\max}\right) \qquad \frac{\partial L}{\partial \lambda_{tkm\min}} = \left(-t_{km} + t_{km\min}\right)$$

$$\frac{\partial L}{\partial t_{km}} = \mu_{Pm}\left[\frac{\partial P_m}{\partial t_{km}}\right] + \mu_{Qm}\left[\frac{\partial Q_m}{\partial t_{km}}\right] + \mu_{Pk}\left[\frac{\partial P_k}{\partial t_{km}}\right] + \mu_{Qk}\left[\frac{\partial Q_k}{\partial t_{km}}\right] + \left(\lambda_{Skm}\left[\frac{\partial |S_{km}|^2}{\partial t_{km}}\right]\right) + \left(k\left[\frac{\partial |S_{km}|^2}{\partial t_{km}}\right]\right) + \left(\lambda_{tkm\max}\right) + \left(-\lambda_{tkm\min}\right)$$

Gradient terms due to phase shifting transformers

$$\frac{\partial L}{\partial \lambda_{\alpha km\max}} = \left(\alpha_{km} - \alpha_{km\max}\right) \qquad \frac{\partial L}{\partial \lambda_{\alpha km\min}} = \left(-\alpha_{km} + \alpha_{km\min}\right)$$

$$\frac{\partial L}{\partial \alpha_{km}} = \mu_{Pm}\left[\frac{\partial P_m}{\partial \alpha_{km}}\right] + \mu_{Qm}\left[\frac{\partial Q_m}{\partial \alpha_{km}}\right] + \mu_{Pk}\left[\frac{\partial P_k}{\partial \alpha_{km}}\right] + \mu_{Qk}\left[\frac{\partial Q_k}{\partial \alpha_{km}}\right] + \left(\lambda_{Skm}\left[\frac{\partial |S_{km}|^2}{\partial \alpha_{km}}\right]\right) + \left(k\left[\frac{\partial |S_{km}|^2}{\partial \alpha_{km}}\right]\right) + \left(\lambda_{\alpha km\max}\right) + \left(-\lambda_{\alpha km\min}\right)$$

APPENDIX C. CALCULATION OF THE HESSIAN OF THE LAGRANGIAN

Appendix C contains a list of all the terms that make up the Hessian of the Lagrangian for the OPF. The listing is organized by those equations or constraints which result in the addition of the Hessian term.

Note: The terms that are shown surrounded by parenthesis, (), are not always part of the Hessian. They are dependent on those inequality constraints being enforced.

Note: Many terms are surrounded by brackets, []. Appendix E contains a further explanation of the calculation of these terms.

Hessian term due to generator cost curves (the objective function)

$$\frac{\partial^2 L}{\partial P_{Gi}{}^2} = 2c_i$$

Hessian terms due to the power flow equations

$$\frac{\partial^2 L}{\partial x \partial y} = \sum_k \left\{ \mu_{Pk} \left[\frac{\partial^2 P_k}{\partial x \partial y} \right] + \mu_{Qk} \left[\frac{\partial^2 Q_k}{\partial x \partial y} \right] \right\} \quad \text{where } x \text{ and } y = V_i, V_j, \delta_i, \text{ or } \delta_j$$

$$\frac{\partial^2 L}{\partial V_i \partial \mu_{Pk}} = \left[\frac{\partial P_k}{\partial V_i} \right] \qquad \frac{\partial^2 L}{\partial V_i \partial \mu_{Qk}} = \left[\frac{\partial Q_k}{\partial V_i} \right]$$

$$\frac{\partial^2 L}{\partial \delta_i \partial \mu_{Pk}} = \left[\frac{\partial P_k}{\partial \delta_i} \right] \qquad \frac{\partial^2 L}{\partial \delta_i \partial \mu_{Qk}} = \left[\frac{\partial Q_k}{\partial \delta_i} \right]$$

$$\frac{\partial^2 L}{\partial P_{Gk} \partial \mu_{Pk}} = -1$$

Hessian terms due to generator voltage set points

$$\frac{\partial^2 L}{\partial V_i \partial \mu_{viset}} = +1$$

Hessian terms due to maximum and minimum generator power output

$$\frac{\partial^2 L}{\partial P_{Gi} \partial \lambda_{PGil}} = (-1) \qquad \frac{\partial^2 L}{\partial P_{Gi} \partial \lambda_{PGih}} = (+1)$$

Hessian terms due to hard transmission line constraints

$$\frac{\partial^2 L}{\partial \lambda_{Skm} \partial x} = \left(\left[\frac{\partial \left| S_{km} \right|^2}{\partial x} \right] \right) \quad \text{where } x = V_k, V_m, \delta_k, \text{ or } \delta_m$$

$$\frac{\partial^2 L}{\partial x \partial y} = \left(\lambda_{Skm} \left[\frac{\partial^2 \left| S_{km} \right|^2}{\partial x \partial y} \right] \right) \quad \text{where } x \text{ and } y = V_k, V_m, \delta_k, \text{ or } \delta_m$$

Hessian terms due to soft transmission line constraints

$$\frac{\partial^2 L}{\partial x \partial y} = \left(2k \left(\left| S_{km} \right|^2 - \left| S_{km\max} \right|^2 \right) \left[\frac{\partial^2 \left| S_{km} \right|^2}{\partial x \partial y} \right] + 2k \left[\frac{\partial \left| S_{km} \right|^2}{\partial x} \right] \left[\frac{\partial \left| S_{km} \right|^2}{\partial y} \right] \right)$$

where $x = V_k, V_m, \delta_k, \text{ or } \delta_m$

Hessian terms due to area interchange constraints

$$\frac{\partial^2 L}{\partial \mu_{\text{int}} \partial x} = \sum_{\text{tie lines}} \left[\frac{\partial P_{km}}{\partial x} \right] \qquad \frac{\partial^2 L}{\partial x \partial y} = \mu_{\text{int}} \sum_{\text{tie lines}} \left[\frac{\partial^2 P_{km}}{\partial x \partial y} \right]$$

where x and $y = V_k, V_m, \delta_k, \text{or } \delta_m$

Hessian terms due to hard voltage constraints

$$\frac{\partial^2 L}{\partial V_i \partial \lambda_{vih}} = (+1) \qquad \frac{\partial^2 L}{\partial V_i \partial \lambda_{vil}} = (-1) \qquad \frac{\partial^2 L}{\partial V_i^2} = (0)$$

Hessian terms due to soft voltage constraints

$$\frac{\partial^2 L}{\partial V_i^2} = (2k)$$

Hessian terms due to tap changing transformers

$$\frac{\partial^2 L}{\partial t_{km} \partial x} = \mu_{Pm}\left[\frac{\partial^2 P_m}{\partial t_{km} \partial x}\right] + \mu_{Qm}\left[\frac{\partial^2 Q_m}{\partial t_{km} \partial x}\right] + \mu_{Pk}\left[\frac{\partial^2 P_k}{\partial t_{km} \partial x}\right] + \mu_{Qk}\left[\frac{\partial^2 Q_k}{\partial t_{km} \partial x}\right] + \left(\lambda_{Skm}\left[\frac{\partial^2 |S_{km}|^2}{\partial t_{km} \partial x}\right]\right) + \left(k\left[\frac{\partial^2 |S_{km}|^2}{\partial t_{km} \partial x}\right]\right) \quad \text{where } x = V_k, V_m, \delta_k, \text{ or } \delta_m$$

$$\frac{\partial^2 L}{\partial \lambda_{tkm\max} \partial t_{km}} = (+1) \qquad \frac{\partial^2 L}{\partial \lambda_{tkm\min} \partial t_{km}} = (-1)$$

$$\frac{\partial^2 L}{\partial t_{km} \partial \mu_{Pm}} = \left[\frac{\partial P_m}{\partial t_{km}}\right] \qquad \frac{\partial^2 L}{\partial t_{km} \partial \mu_{Qm}} = \left[\frac{\partial Q_m}{\partial t_{km}}\right]$$

$$\frac{\partial^2 L}{\partial t_{km} \partial \mu_{Pk}} = \left[\frac{\partial P_k}{\partial t_{km}}\right] \qquad \frac{\partial^2 L}{\partial t_{km} \partial \mu_{Qk}} = \left[\frac{\partial Q_k}{\partial t_{km}}\right]$$

$$\frac{\partial^2 L}{\partial t_{km} \partial \lambda_{Skm}} = \left(\left[\frac{\partial |S_{km}|^2}{\partial t_{km}}\right] \text{ or } \left[\frac{\partial |S_{mk}|^2}{\partial t_{km}}\right]\right); \text{ depending on which end of the line is metered}$$

$$\frac{\partial^2 L}{\partial t_{km} \partial \mu_{\text{int}}} = \left[\frac{\partial P_{\text{int}}}{\partial t_{km}}\right] = \left[\frac{\partial P_{km}}{\partial t_{km}}\right] \text{ or } \left[\frac{\partial P_{km}}{\partial t_{km}}\right]; \text{ depending on which end of the line is metered}$$

Hessian terms due to phase shifting transformers

$$\frac{\partial^2 L}{\partial \alpha_{km} \partial x} = \mu_{Pm}\left[\frac{\partial^2 P_m}{\partial \alpha_{km} \partial x}\right] + \mu_{Qm}\left[\frac{\partial^2 Q_m}{\partial \alpha_{km} \partial x}\right] + \mu_{Pk}\left[\frac{\partial^2 P_k}{\partial \alpha_{km} \partial x}\right] + \mu_{Qk}\left[\frac{\partial^2 Q_k}{\partial \alpha_{km} \partial x}\right] + \left(\lambda_{Skm}\left[\frac{\partial^2 |S_{km}|^2}{\partial \alpha_{km} \partial x}\right]\right) + \left(k\left[\frac{\partial^2 |S_{km}|^2}{\partial \alpha_{km} \partial x}\right]\right) \quad \text{where } x = V_k, V_m, \delta_k, \text{ or } \delta_m$$

$$\frac{\partial^2 L}{\partial \lambda_{\alpha km \max} \partial \alpha_{km}} = (+1) \qquad \frac{\partial^2 L}{\partial \lambda_{\alpha km \min} \partial \alpha_{km}} = (-1)$$

$$\frac{\partial^2 L}{\partial \alpha_{km} \partial \mu_{Pm}} = \left[\frac{\partial P_m}{\partial \alpha_{km}}\right] \qquad \frac{\partial^2 L}{\partial \alpha_{km} \partial \mu_{Qm}} = \left[\frac{\partial Q_m}{\partial \alpha_{km}}\right]$$

$$\frac{\partial^2 L}{\partial \alpha_{km} \partial \mu_{Pk}} = \left[\frac{\partial P_k}{\partial \alpha_{km}}\right] \qquad \frac{\partial^2 L}{\partial \alpha_{km} \partial \mu_{Qk}} = \left[\frac{\partial Q_k}{\partial \alpha_{km}}\right]$$

$$\frac{\partial^2 L}{\partial \alpha_{km} \partial \lambda_{Skm}} = \left(\left[\frac{\partial |S_{km}|^2}{\partial \alpha_{km}}\right] \text{ or } \left[\frac{\partial |S_{mk}|^2}{\partial \alpha_{km}}\right]\right); \quad \text{depending on which end of the line is metered}$$

$$\frac{\partial^2 L}{\partial \alpha_{km} \partial \mu_{\text{int}}} = \left[\frac{\partial P_{\text{int}}}{\partial \alpha_{km}}\right] = \left[\frac{\partial P_{km}}{\partial \alpha_{km}}\right] \text{ or } \left[\frac{\partial P_{km}}{\partial \alpha_{km}}\right]; \quad \text{depending on which end of the line is metered}$$

APPENDIX D. SUMMARY OF DERIVATIVE CALCULATIONS

In Appendices B and C, many partial derivatives left uncalculated. These partial derivatives are summarized in Appendix D. The listing is organized by the equations being differentiated.

Calculation of partial derivatives of the net power and reactive power injections.

$$P_k = V_k \sum_{m=1}^{N} \left[V_m \left[g_{km} \cos\left(\delta_k - \delta_m\right) + b_{km} \sin\left(\delta_k - \delta_m\right) \right] \right] - P_{Gk} + P_{Lk}$$

$$Q_k = V_k \sum_{m=1}^{N} \left[V_m \left[g_{km} \sin\left(\delta_k - \delta_m\right) - b_{km} \cos\left(\delta_k - \delta_m\right) \right] \right] - Q_{Gk} + Q_{Lk} \qquad \text{(D.1)}$$

where g_{km} and b_{km} are elements of the real and imaginary parts of the network admittance matrix

From Equation (D.1), the following partial derivatives can be found

$\left[\frac{\partial P_k}{\partial \delta_i}\right], \left[\frac{\partial Q_k}{\partial \delta_i}\right], \left[\frac{\partial P_k}{\partial V_i}\right]$, and $\left[\frac{\partial Q_k}{\partial V_i}\right]$ are elements of the familiar power system Jacobian matrix

$$\left[\frac{\partial^2 P_k}{\partial V_k{}^2}\right] = 2 g_{kk}$$

$$\left[\frac{\partial^2 P_k}{\partial V_m{}^2}\right] = 0$$

$$\left[\frac{\partial^2 P_k}{\partial V_k \partial V_m}\right] = g_{km} \cos\left(\delta_k - \delta_m\right) + b_{km} \sin\left(\delta_k - \delta_m\right)$$

$$\left[\frac{\partial^2 P_k}{\partial \delta_k{}^2}\right] = -V_k \sum_{n=1}^{\text{all busses}} \left[V_n \left[g_{kn} \cos\left(\delta_k - \delta_n\right) + b_{kn} \sin\left(\delta_k - \delta_n\right) \right] \right]$$

$$\left[\frac{\partial^2 P_k}{\partial \delta_k \partial \delta_m}\right] = V_k V_m \left[g_{km} \cos\left(\delta_k - \delta_m\right) + b_{km} \sin\left(\delta_k - \delta_m\right) \right]$$

$$\left[\frac{\partial^2 P_k}{\partial \delta_m{}^2}\right] = V_k V_m\left[-g_{km}\cos\left(\delta_k-\delta_m\right)-b_{km}\sin\left(\delta_k-\delta_m\right)\right]$$

$$\left[\frac{\partial^2 P_k}{\partial V_k \partial \delta_k}\right] = \sum_{\text{n}}^{\text{all busses}}\left\{V_n\left[-g_{kn}\sin\left(\delta_k-\delta_n\right)+b_{kn}\cos\left(\delta_k-\delta_n\right)\right]\right\}$$

$$\left[\frac{\partial^2 P_k}{\partial V_k \partial \delta_m}\right] = V_m\left[g_{km}\sin\left(\delta_k-\delta_m\right)-b_{km}\cos\left(\delta_k-\delta_m\right)\right]$$

$$\left[\frac{\partial^2 P_k}{\partial V_m \partial \delta_k}\right] = V_k\left[-g_{km}\sin\left(\delta_k-\delta_m\right)+b_{km}\cos\left(\delta_k-\delta_m\right)\right]$$

$$\left[\frac{\partial^2 P_k}{\partial V_m \partial \delta_m}\right] = V_k\left[g_{km}\sin\left(\delta_k-\delta_m\right)-b_{km}\cos\left(\delta_k-\delta_m\right)\right]$$

$$\left[\frac{\partial^2 Q_k}{\partial V_k{}^2}\right] = -2b_{kk}$$

$$\left[\frac{\partial^2 Q_k}{\partial V_m{}^2}\right] = 0$$

$$\left[\frac{\partial^2 Q_k}{\partial V_k \partial V_m}\right] = g_{km}\sin\left(\delta_k-\delta_m\right)-b_{km}\cos\left(\delta_k-\delta_m\right)$$

$$\left[\frac{\partial^2 Q_k}{\partial \delta_k{}^2}\right] = -V_k\sum_{n=1}^{\text{all busses}}\left[V_n\left[g_{kn}\sin\left(\delta_k-\delta_n\right)-b_{kn}\cos\left(\delta_k-\delta_n\right)\right]\right]$$

$$\left[\frac{\partial^2 Q_k}{\partial \delta_k \partial \delta_m}\right] = V_k V_m\left[g_{km}\sin\left(\delta_k-\delta_m\right)-b_{km}\cos\left(\delta_k-\delta_m\right)\right]$$

$$\left[\frac{\partial^2 Q_k}{\partial \delta_m{}^2}\right] = V_k V_m\left[-g_{km}\sin\left(\delta_k-\delta_m\right)+b_{km}\cos\left(\delta_k-\delta_m\right)\right]$$

$$\left[\frac{\partial^2 Q_k}{\partial V_k \partial \delta_k}\right] = \sum_{\text{n}}^{\text{all busses}}\left\{V_n\left[g_{kn}\cos\left(\delta_k-\delta_n\right)+b_{kn}\sin\left(\delta_k-\delta_n\right)\right]\right\}$$

$$\left[\frac{\partial^2 Q_k}{\partial V_k \partial \delta_m}\right] = -V_m\left[g_{km}\cos\left(\delta_k - \delta_m\right) + b_{km}\sin\left(\delta_k - \delta_m\right)\right]$$

$$\left[\frac{\partial^2 Q_k}{\partial V_m \partial \delta_k}\right] = V_k\left[g_{km}\cos\left(\delta_k - \delta_m\right) + b_{km}\sin\left(\delta_k - \delta_m\right)\right]$$

$$\left[\frac{\partial^2 Q_k}{\partial V_m \partial \delta_m}\right] = -V_k\left[g_{km}\cos\left(\delta_k - \delta_m\right) + b_{km}\sin\left(\delta_k - \delta_m\right)\right]$$

Calculation of the partial derivatives of the power and reactive power flow between buses.

$$P_{km} = +V_k{}^2 g_{kk} + V_k V_m\left[g_{km}\cos\left(\delta_k - \delta_m\right) + b_{km}\sin\left(\delta_k - \delta_m\right)\right]$$
$$Q_{km} = -V_k{}^2 b_{kk} + V_k V_m\left[g_{km}\sin\left(\delta_k - \delta_m\right) - b_{km}\cos\left(\delta_k - \delta_m\right)\right] \qquad \text{(D.2)}$$

where g_{kk}, b_{kk}, g_{km}, and b_{km} are the contributions to the network admittance matrix from the branch between bus k and bus m.

From Equation (D.2), the following partial derivatives can be found

$$\left[\frac{\partial P_{km}}{\partial V_k}\right] = 2V_k g_{kk} + V_m\left[g_{km}\cos\left(\delta_k - \delta_m\right) + b_{km}\sin\left(\delta_k - \delta_m\right)\right]$$

$$\left[\frac{\partial P_{km}}{\partial V_m}\right] = V_k\left[g_{km}\cos\left(\delta_k - \delta_m\right) + b_{km}\sin\left(\delta_k - \delta_m\right)\right]$$

$$\left[\frac{\partial P_{km}}{\partial \delta_k}\right] = V_k V_m\left[-g_{km}\sin\left(\delta_k - \delta_m\right) + b_{km}\cos\left(\delta_k - \delta_m\right)\right]$$

$$\left[\frac{\partial P_{km}}{\partial \delta_m}\right] = V_k V_m\left[g_{km}\sin\left(\delta_k - \delta_m\right) - b_{km}\cos\left(\delta_k - \delta_m\right)\right]$$

$$\left[\frac{\partial Q_{km}}{\partial V_k}\right] = -2V_k b_{kk} + V_m\left[g_{km}\sin\left(\delta_k - \delta_m\right) - b_{km}\cos\left(\delta_k - \delta_m\right)\right]$$

$$\left[\frac{\partial Q_{km}}{\partial V_m}\right] = V_k\left[g_{km}\sin\left(\delta_k - \delta_m\right) - b_{km}\cos\left(\delta_k - \delta_m\right)\right]$$

$$\left[\frac{\partial Q_{km}}{\partial \delta_k}\right] = V_k V_m\left[g_{km}\cos\left(\delta_k - \delta_m\right) + b_{km}\sin\left(\delta_k - \delta_m\right)\right]$$

$$\left[\frac{\partial Q_{km}}{\partial \delta_m}\right] = V_k V_m\left[-g_{km}\cos\left(\delta_k - \delta_m\right) - b_{km}\sin\left(\delta_k - \delta_m\right)\right]$$

$$\left[\frac{\partial^2 P_{km}}{\partial V_k^{\,2}}\right] = 2g_{kk}$$

$$\left[\frac{\partial^2 P_{km}}{\partial V_k \partial V_m}\right] = g_{km}\cos\left(\delta_k - \delta_m\right) + b_{km}\sin\left(\delta_k - \delta_m\right)$$

$$\left[\frac{\partial^2 P_{km}}{\partial V_m^{\,2}}\right] = 0$$

$$\left[\frac{\partial^2 P_{km}}{\partial \delta_k^{\,2}}\right] = -V_k V_m\left[g_{km}\cos\left(\delta_k - \delta_m\right) + b_{km}\sin\left(\delta_k - \delta_m\right)\right]$$

$$\left[\frac{\partial^2 P_{km}}{\partial \delta_k \partial \delta_m}\right] = V_k V_m\left[g_{km}\cos\left(\delta_k - \delta_m\right) + b_{km}\sin\left(\delta_k - \delta_m\right)\right]$$

$$\left[\frac{\partial^2 P_{km}}{\partial \delta_m^{\,2}}\right] = -V_k V_m\left[g_{km}\cos\left(\delta_k - \delta_m\right) + b_{km}\sin\left(\delta_k - \delta_m\right)\right]$$

$$\left[\frac{\partial^2 P_{km}}{\partial V_k \partial \delta_k}\right] = V_m\left[-g_{km}\sin\left(\delta_k - \delta_m\right) + b_{km}\cos\left(\delta_k - \delta_m\right)\right]$$

$$\left[\frac{\partial^2 P_{km}}{\partial V_k \partial \delta_m}\right] = V_m\left[g_{km}\sin\left(\delta_k - \delta_m\right) - b_{km}\cos\left(\delta_k - \delta_m\right)\right]$$

$$\left[\frac{\partial^2 P_{km}}{\partial V_m \partial \delta_k}\right] = V_k\left[-g_{km}\sin\left(\delta_k - \delta_m\right) + b_{km}\cos\left(\delta_k - \delta_m\right)\right]$$

$$\left[\frac{\partial^2 P_{km}}{\partial V_m \partial \delta_m}\right] = V_k\left[g_{km}\sin\left(\delta_k-\delta_m\right)-b_{km}\cos\left(\delta_k-\delta_m\right)\right]$$

$$\left[\frac{\partial^2 Q_{km}}{\partial V_k{}^2}\right] = -2b_{kk}$$

$$\left[\frac{\partial^2 Q_{km}}{\partial V_k \partial V_m}\right] = g_{km}\sin\left(\delta_k-\delta_m\right)-b_{km}\cos\left(\delta_k-\delta_m\right)$$

$$\left[\frac{\partial^2 Q_{km}}{\partial V_m{}^2}\right] = 0$$

$$\left[\frac{\partial^2 Q_{km}}{\partial \delta_k{}^2}\right] = -V_k V_m\left[g_{km}\sin\left(\delta_k-\delta_m\right)-b_{km}\cos\left(\delta_k-\delta_m\right)\right]$$

$$\left[\frac{\partial^2 Q_{km}}{\partial \delta_k \partial \delta_m}\right] = V_k V_m\left[g_{km}\sin\left(\delta_k-\delta_m\right)-b_{km}\cos\left(\delta_k-\delta_m\right)\right]$$

$$\left[\frac{\partial^2 Q_{km}}{\partial \delta_m{}^2}\right] = -V_k V_m\left[g_{km}\sin\left(\delta_k-\delta_m\right)-b_{km}\cos\left(\delta_k-\delta_m\right)\right]$$

$$\left[\frac{\partial^2 Q_{km}}{\partial V_k \partial \delta_k}\right] = V_m\left[g_{km}\cos\left(\delta_k-\delta_m\right)+b_{km}\sin\left(\delta_k-\delta_m\right)\right]$$

$$\left[\frac{\partial^2 Q_{km}}{\partial V_k \partial \delta_m}\right] = V_m\left[-g_{km}\cos\left(\delta_k-\delta_m\right)-b_{km}\sin\left(\delta_k-\delta_m\right)\right]$$

$$\left[\frac{\partial^2 Q_{km}}{\partial V_m \partial \delta_k}\right] = V_k\left[+g_{km}\cos\left(\delta_k-\delta_m\right)+b_{km}\sin\left(\delta_k-\delta_m\right)\right]$$

$$\left[\frac{\partial^2 Q_{km}}{\partial V_m \partial \delta_m}\right] = V_k\left[-g_{km}\cos\left(\delta_k-\delta_m\right)-b_{km}\sin\left(\delta_k-\delta_m\right)\right]$$

Calculation of the partial derivatives of the square of the MVA flow on a line, $|S_{km}|^2$

$$\left|S_{km}\right|^2 = P_{km}{}^2 + Q_{km}{}^2 \tag{D.3}$$

From Equation (D.3), the following partial derivative can be found

$$\left[\frac{\partial\left|S_{km}\right|^2}{\partial x}\right] = 2P_{km}\left[\frac{\partial P_{km}}{\partial x}\right] + 2Q_{km}\left[\frac{\partial Q_{km}}{\partial x}\right] \qquad \text{where } x = V_k, V_m, \delta_k, \text{ or } \delta_m$$

Equation (D.3) can also be simplified to the following

$$\left|S_{km}\right|^2 = V_k{}^4 y_{kk}{}^2 + V_k{}^2 V_m{}^2 y_{km}{}^2 + 2V_k{}^3 V_m y_{km} y_{kk} \cos\left(\delta_k - \delta_m + \delta_{kk} - \delta_{km}\right) \tag{D.4}$$

where $g_{kk} + jb_{kk} = y_{kk} e^{j\delta_{kk}}$ and $g_{km} + jb_{km} = y_{km} e^{j\delta_{km}}$

From Equation (D.4), the following partial derivatives can be found

$$\left[\frac{\partial^2\left|S_{km}\right|^2}{\partial\delta_k{}^2}\right] = -2V_k{}^3 V_m y_{km} y_{kk} \cos\left(\delta_k - \delta_m + \delta_{kk} - \delta_{km}\right)$$

$$\left[\frac{\partial^2\left|S_{km}\right|^2}{\partial\delta_k \partial\delta_m}\right] = 2V_k{}^3 V_m y_{km} y_{kk} \cos\left(\delta_k - \delta_m + \delta_{kk} - \delta_{km}\right)$$

$$\left[\frac{\partial^2\left|S_{km}\right|^2}{\partial\delta_m{}^2}\right] = -2V_k{}^3 V_m y_{km} y_{kk} \cos\left(\delta_k - \delta_m + \delta_{kk} - \delta_{km}\right)$$

$$\left[\frac{\partial^2\left|S_{km}\right|^2}{\partial V_k{}^2}\right] = 12V_k{}^2 y_{kk}{}^2 + 2V_m{}^2 y_{km}{}^2 + 12V_k V_m y_{km} y_{kk} \cos\left(\delta_k - \delta_m + \delta_{kk} - \delta_{km}\right)$$

$$\left[\frac{\partial^2\left|S_{km}\right|^2}{\partial V_k \partial V_m}\right] = 4V_k V_m y_{km}{}^2 + 6V_k{}^2 y_{km} y_{kk} \cos\left(\delta_k - \delta_m + \delta_{kk} - \delta_{km}\right)$$

$$\left[\frac{\partial^2\left|S_{km}\right|^2}{\partial V_m{}^2}\right] = 2V_k{}^2 y_{km}{}^2$$

$$\left[\frac{\partial^2\left|S_{km}\right|^2}{\partial V_k \partial\delta_k}\right] = -6V_k{}^2 V_m y_{km} y_{kk} \sin\left(\delta_k - \delta_m + \delta_{kk} - \delta_{km}\right)$$

$$\left[\frac{\partial^2 |S_{km}|^2}{\partial V_k \partial \delta_m}\right] = 6V_k{}^2 V_m y_{km} y_{kk} \sin\left(\delta_k - \delta_m + \delta_{kk} - \delta_{km}\right)$$

$$\left[\frac{\partial^2 |S_{km}|^2}{\partial V_m \partial \delta_k}\right] = -2V_k{}^3 y_{km} y_{kk} \sin\left(\delta_k - \delta_m + \delta_{kk} - \delta_{km}\right)$$

$$\left[\frac{\partial^2 |S_{km}|^2}{\partial V_m \partial \delta_m}\right] = 2V_k{}^3 y_{km} y_{kk} \sin\left(\delta_k - \delta_m + \delta_{kk} - \delta_{km}\right)$$

Calculation of partial derivatives with respect to tap ratio and phase shift variables

Before beginning calculation of the partial derivative with respect to tap ratio and phase shift variables, first consider what equations they affect. In the modeling of power systems, tap ratios and phase shifts are typically represented as alterations to the network admittance matrix. Figure D.1 shows the model for a transformer with tap changing and/or phase shifting capabilities.

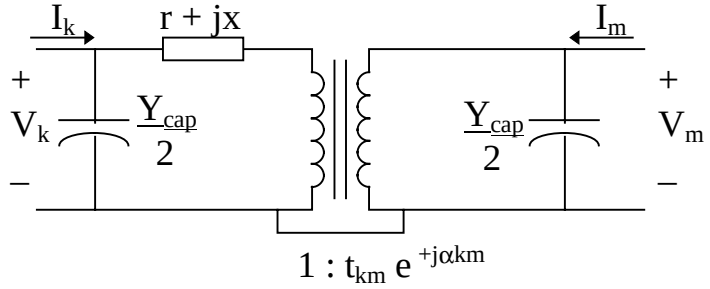

Figure D.1 Transformer Model

Using this model, the entries in the network admittance matrix due to the transformer can be found as in the book by Grainger [20, pp. 361-362].

$$\begin{bmatrix} I_k \\ \cdots \\ I_m \end{bmatrix} = \begin{matrix} \\ \text{row k} \\ \text{row m} \end{matrix} \underbrace{\begin{matrix} \text{col k} & \text{col m} \\ \begin{bmatrix} y + \frac{Y_{cap}}{2} & -\frac{e^{-j\alpha_{km}}}{t_{km}} y \\ -\frac{e^{+j\alpha_{km}}}{t_{km}} y & \frac{1}{t_{km}^{\,2}} y + \frac{Y_{cap}}{2} \end{bmatrix} \end{matrix}}_{Y} \begin{bmatrix} V_k \\ \cdots \\ V_m \end{bmatrix} \quad \text{where } y = \frac{1}{r + jx} = g + jb$$

From this model, the following derivatives are defined.

$$\frac{\partial [Y]}{\partial t_{km}} = \begin{bmatrix} \frac{\partial Y_{kk}}{\partial t_{km}} & \frac{\partial Y_{km}}{\partial t_{km}} \\ \frac{\partial Y_{mk}}{\partial t_{km}} & \frac{\partial Y_{mm}}{\partial t_{km}} \end{bmatrix} = \begin{bmatrix} 0 & \frac{e^{-j\alpha_{km}}}{t_{km}^{\,2}} y \\ \frac{e^{+j\alpha_{km}}}{t_{km}^{\,2}} y & \frac{-2}{t_{km}^{\,3}} y \end{bmatrix} = \begin{bmatrix} 0 & \frac{-1}{t_{km}} Y_{km} \\ \frac{-1}{t_{km}} Y_{mk} & \frac{-2}{t_{km}} Y_{mm} \end{bmatrix}$$

$$\frac{\partial^2 [Y]}{\partial t_{km}^{\,2}} = \begin{bmatrix} \frac{\partial^2 Y_{kk}}{\partial t_{km}^{\,2}} & \frac{\partial^2 Y_{km}}{\partial t_{km}^{\,2}} \\ \frac{\partial^2 Y_{mk}}{\partial t_{km}^{\,2}} & \frac{\partial^2 Y_{mm}}{\partial t_{km}^{\,2}} \end{bmatrix} = \begin{bmatrix} 0 & \frac{-2e^{-j\alpha_{km}}}{t_{km}^{\,3}} y \\ \frac{-2e^{+j\alpha_{km}}}{t_{km}^{\,3}} y & \frac{6}{t_{km}^{\,4}} y \end{bmatrix} = \begin{bmatrix} 0 & \frac{2}{t_{km}^{\,2}} Y_{km} \\ \frac{2}{t_{km}^{\,2}} Y_{mk} & \frac{6}{t_{km}^{\,2}} Y_{mm} \end{bmatrix}$$

$$\frac{\partial [Y]}{\partial \alpha_{km}} = \begin{bmatrix} \frac{\partial Y_{kk}}{\partial \alpha_{km}} & \frac{\partial Y_{km}}{\partial \alpha_{km}} \\ \frac{\partial Y_{mk}}{\partial \alpha_{km}} & \frac{\partial Y_{mm}}{\partial \alpha_{km}} \end{bmatrix} = \begin{bmatrix} 0 & j\frac{e^{-j\alpha_{km}}}{t_{km}} y \\ j\frac{-e^{+j\alpha_{km}}}{t_{km}} y & 0 \end{bmatrix} = \begin{bmatrix} 0 & -jY_{km} \\ jY_{mk} & 0 \end{bmatrix} = \begin{bmatrix} 0 & -jg_{km} + b_{km} \\ jg_{mk} - b_{mk} & 0 \end{bmatrix}$$

$$\frac{\partial^2 [Y]}{\partial \alpha_{km}^{\,2}} = \begin{bmatrix} \frac{\partial^2 Y_{kk}}{\partial \alpha_{km}^{\,2}} & \frac{\partial^2 Y_{km}}{\partial \alpha_{km}^{\,2}} \\ \frac{\partial^2 Y_{mk}}{\partial \alpha_{km}^{\,2}} & \frac{\partial^2 Y_{mm}}{\partial \alpha_{km}^{\,2}} \end{bmatrix} = \begin{bmatrix} 0 & \frac{e^{-j\alpha_{km}}}{t_{km}} y \\ \frac{e^{+j\alpha_{km}}}{t_{km}} y & 0 \end{bmatrix} = \begin{bmatrix} 0 & -Y_{km} \\ -Y_{mk} & 0 \end{bmatrix} = \begin{bmatrix} 0 & -g_{km} - jb_{km} \\ -g_{mk} - jb_{mk} & 0 \end{bmatrix}$$

From these equations, the partial derivatives of elements of the network admittance matrix with respect to tap ratio and phase shift angle can be summarized as below.

$$\frac{\partial g_{kk}}{\partial t_{km}} = 0 \qquad \frac{\partial g_{km}}{\partial t_{km}} = -\frac{g_{km}}{t_{km}} \qquad \frac{\partial b_{kk}}{\partial t_{km}} = 0 \qquad \frac{\partial b_{km}}{\partial t_{km}} = -\frac{b_{km}}{t_{km}}$$

$$\frac{\partial g_{mk}}{\partial t_{km}} = -\frac{g_{mk}}{t_{km}} \qquad \frac{\partial g_{mm}}{\partial t_{km}} = -\frac{2g_{mm}}{t_{km}} \qquad \frac{\partial b_{mk}}{\partial t_{km}} = -\frac{b_{mk}}{t_{km}} \qquad \frac{\partial b_{mm}}{\partial t_{km}} = -\frac{2b_{mm}}{t_{km}}$$

$$\frac{\partial^2 g_{kk}}{\partial t_{km}^{\,2}} = 0 \qquad \frac{\partial^2 g_{km}}{\partial t_{km}^{\,2}} = \frac{2g_{km}}{t_{km}^{\,2}} \qquad \frac{\partial^2 b_{kk}}{\partial t_{km}^{\,2}} = 0 \qquad \frac{\partial^2 b_{km}}{\partial t_{km}^{\,2}} = \frac{2b_{km}}{t_{km}^{\,2}}$$

$$\frac{\partial^2 g_{mk}}{\partial t_{km}^{\,2}} = \frac{2g_{mk}}{t_{km}^{\,2}} \qquad \frac{\partial^2 g_{mm}}{\partial t_{km}^{\,2}} = \frac{6g_{mm}}{t_{km}^{\,2}} \qquad \frac{\partial^2 b_{mk}}{\partial t_{km}^{\,2}} = \frac{2b_{mk}}{t_{km}^{\,2}} \qquad \frac{\partial^2 b_{mm}}{\partial t_{km}^{\,2}} = \frac{6b_{mm}}{t_{km}^{\,2}}$$

$$\frac{\partial g_{kk}}{\partial \alpha_{km}} = 0 \qquad \frac{\partial g_{km}}{\partial \alpha_{km}} = b_{km} \qquad \frac{\partial b_{kk}}{\partial \alpha_{km}} = 0 \qquad \frac{\partial b_{km}}{\partial \alpha_{km}} = -g_{km}$$

$$\frac{\partial g_{mk}}{\partial \alpha_{km}} = -b_{mk} \qquad \frac{\partial g_{mm}}{\partial \alpha_{km}} = 0 \qquad \frac{\partial b_{mk}}{\partial \alpha_{km}} = g_{mk} \qquad \frac{\partial b_{mm}}{\partial \alpha_{km}} = 0$$

$$\frac{\partial^2 g_{kk}}{\partial \alpha_{km}^{\,2}} = 0 \qquad \frac{\partial^2 g_{km}}{\partial \alpha_{km}^{\,2}} = -g_{km} \qquad \frac{\partial^2 b_{kk}}{\partial \alpha_{km}^{\,2}} = 0 \qquad \frac{\partial^2 b_{km}}{\partial \alpha_{km}^{\,2}} = -b_{km}$$

$$\frac{\partial^2 g_{mk}}{\partial \alpha_{km}^{\,2}} = -g_{mk} \qquad \frac{\partial^2 g_{mm}}{\partial \alpha_{km}^{\,2}} = 0 \qquad \frac{\partial^2 b_{mk}}{\partial \alpha_{km}^{\,2}} = -b_{mk} \qquad \frac{\partial^2 b_{mm}}{\partial \alpha_{km}^{\,2}} = 0$$

The equations that have to be differentiated are of the form

$$w(\bullet, t_{km}) = u(\bullet) b_{km}(t_{km}) + v(\bullet) g_{km}(t_{km}).$$

Therefore, the derivatives that need to be calculated may be found as follows.

$$\frac{\partial w}{\partial t_{km}} = u\frac{\partial b_{km}}{\partial t_{km}} + v\frac{\partial g_{km}}{\partial t_{km}} \qquad \frac{\partial^2 w}{\partial t_{km}^{\,2}} = u\frac{\partial^2 b_{km}}{\partial t_{km}^{\,2}} + v\frac{\partial^2 g_{km}}{\partial t_{km}^{\,2}}$$

$$\frac{\partial^2 w}{\partial t_{km}\partial x} = \frac{\partial}{\partial x}\left(u\frac{\partial b_{km}}{\partial t_{km}} + v\frac{\partial g_{km}}{\partial t_{km}}\right) \quad \text{where } x = V_k, V_m, \delta_k, \text{ or } \delta_k$$

Using this process, the following partial derivatives with respect to tap ratio can be found.

$$\left[\frac{\partial P_k}{\partial t_{km}}\right] = \left[\frac{\partial P_{km}}{\partial t_{km}}\right] = -\frac{V_k V_m}{t_{km}}\left[g_{km}\cos(\delta_k - \delta_m) + b_{km}\sin(\delta_k - \delta_m)\right]$$

$$\left[\frac{\partial Q_k}{\partial t_{km}}\right] = \left[\frac{\partial Q_{km}}{\partial t_{km}}\right] = -\frac{V_k V_m}{t_{km}}\left[g_{km}\sin(\delta_k - \delta_m) - b_{km}\cos(\delta_k - \delta_m)\right]$$

$$\left[\frac{\partial P_m}{\partial t_{km}}\right]=\left[\frac{\partial P_{mk}}{\partial t_{km}}\right]=-\frac{V_m}{t_{km}}\left\{2V_m g_{mm}+V_k\left[g_{mk}\cos\left(\delta_m-\delta_k\right)+b_{mk}\sin\left(\delta_m-\delta_k\right)\right]\right\}$$

$$\left[\frac{\partial Q_m}{\partial t_{km}}\right]=\left[\frac{\partial Q_{mk}}{\partial t_{km}}\right]=-\frac{V_m}{t_{km}}\left\{-2V_m b_{mm}+V_k\left[g_{mk}\sin\left(\delta_m-\delta_k\right)-b_{mk}\cos\left(\delta_m-\delta_k\right)\right]\right\}$$

$$\left[\frac{\partial^2 P_k}{\partial t_{km}^{\,2}}\right]=\left[\frac{\partial^2 P_{km}}{\partial t_{km}^{\,2}}\right]=\frac{2V_k V_m}{t_{km}^{\,2}}\left[g_{km}\cos\left(\delta_k-\delta_m\right)+b_{km}\sin\left(\delta_k-\delta_m\right)\right]$$

$$\left[\frac{\partial^2 Q_k}{\partial t_{km}^{\,2}}\right]=\left[\frac{\partial^2 Q_{km}}{\partial t_{km}^{\,2}}\right]=\frac{2V_k V_m}{t_{km}^{\,2}}\left[g_{km}\sin\left(\delta_k-\delta_m\right)-b_{km}\cos\left(\delta_k-\delta_m\right)\right]$$

$$\left[\frac{\partial^2 P_m}{\partial t_{km}^{\,2}}\right]=\left[\frac{\partial^2 P_{mk}}{\partial t_{km}^{\,2}}\right]=\frac{2V_m}{t_{km}^{\,2}}\left\{3V_m g_{mm}+V_k\left[g_{mk}\cos\left(\delta_m-\delta_k\right)+b_{mk}\sin\left(\delta_m-\delta_k\right)\right]\right\}$$

$$\left[\frac{\partial^2 Q_m}{\partial t_{km}^{\,2}}\right]=\left[\frac{\partial^2 Q_{mk}}{\partial t_{km}^{\,2}}\right]=\frac{2V_m}{t_{km}^{\,2}}\left\{-3V_m b_{mm}+V_k\left[g_{mk}\sin\left(\delta_m-\delta_k\right)-b_{mk}\cos\left(\delta_m-\delta_k\right)\right]\right\}$$

$$\left[\frac{\partial^2 P_k}{\partial t_{km}\partial V_k}\right]=\left[\frac{\partial^2 P_{km}}{\partial t_{km}\partial V_k}\right]=-\frac{V_m}{t_{km}}\left[g_{km}\cos\left(\delta_k-\delta_m\right)+b_{km}\sin\left(\delta_k-\delta_m\right)\right]$$

$$\left[\frac{\partial^2 P_k}{\partial t_{km}\partial V_m}\right]=\left[\frac{\partial^2 P_{km}}{\partial t_{km}\partial V_m}\right]=-\frac{V_k}{t_{km}}\left[g_{km}\cos\left(\delta_k-\delta_m\right)+b_{km}\sin\left(\delta_k-\delta_m\right)\right]$$

$$\left[\frac{\partial^2 P_k}{\partial t_{km}\partial \delta_k}\right]=\left[\frac{\partial^2 P_{km}}{\partial t_{km}\partial \delta_k}\right]=-\frac{V_k V_m}{t_{km}}\left[-g_{km}\sin\left(\delta_k-\delta_m\right)+b_{km}\cos\left(\delta_k-\delta_m\right)\right]$$

$$\left[\frac{\partial^2 P_k}{\partial t_{km}\partial \delta_m}\right]=\left[\frac{\partial^2 P_{km}}{\partial t_{km}\partial \delta_m}\right]=-\frac{V_k V_m}{t_{km}}\left[g_{km}\sin\left(\delta_k-\delta_m\right)-b_{km}\cos\left(\delta_k-\delta_m\right)\right]$$

$$\left[\frac{\partial^2 Q_k}{\partial t_{km}\partial V_k}\right]=\left[\frac{\partial^2 Q_{km}}{\partial t_{km}\partial V_k}\right]=-\frac{V_m}{t_{km}}\left[g_{km}\sin\left(\delta_k-\delta_m\right)-b_{km}\cos\left(\delta_k-\delta_m\right)\right]$$

$$\left[\frac{\partial^2 Q_k}{\partial t_{km}\partial V_m}\right]=\left[\frac{\partial^2 Q_{km}}{\partial t_{km}\partial V_m}\right]=-\frac{V_k}{t_{km}}\left[g_{km}\sin\left(\delta_k-\delta_m\right)-b_{km}\cos\left(\delta_k-\delta_m\right)\right]$$

$$\left[\frac{\partial^2 Q_k}{\partial t_{km}\partial \delta_k}\right]=\left[\frac{\partial^2 Q_{km}}{\partial t_{km}\partial \delta_k}\right]=-\frac{V_k V_m}{t_{km}}\left[g_{km}\cos\left(\delta_k-\delta_m\right)+b_{km}\sin\left(\delta_k-\delta_m\right)\right]$$

$$\left[\frac{\partial^2 Q_k}{\partial t_{km}\partial \delta_m}\right]=\left[\frac{\partial^2 Q_{km}}{\partial t_{km}\partial \delta_m}\right]=-\frac{V_k V_m}{t_{km}}\left[-g_{km}\cos\left(\delta_k-\delta_m\right)-b_{km}\sin\left(\delta_k-\delta_m\right)\right]$$

$$\left[\frac{\partial^2 P_m}{\partial t_{km}\partial V_k}\right]=\left[\frac{\partial^2 P_{mk}}{\partial t_{km}\partial V_k}\right]=-\frac{V_m}{t_{km}}\left[g_{mk}\cos\left(\delta_m-\delta_k\right)+b_{mk}\sin\left(\delta_m-\delta_k\right)\right]$$

$$\left[\frac{\partial^2 P_m}{\partial t_{km}\partial V_m}\right]=\left[\frac{\partial^2 P_{mk}}{\partial t_{km}\partial V_m}\right]=-\frac{1}{t_{km}}\left\{4V_m g_{mm}+V_k\left[g_{mk}\cos\left(\delta_m-\delta_k\right)+b_{mk}\sin\left(\delta_m-\delta_k\right)\right]\right\}$$

$$\left[\frac{\partial^2 P_m}{\partial t_{km}\partial \delta_k}\right]=\left[\frac{\partial^2 P_{mk}}{\partial t_{km}\partial \delta_k}\right]=-\frac{V_k V_m}{t_{km}}\left[g_{mk}\sin\left(\delta_m-\delta_k\right)-b_{mk}\cos\left(\delta_m-\delta_k\right)\right]$$

$$\left[\frac{\partial^2 P_m}{\partial t_{km}\partial \delta_m}\right]=\left[\frac{\partial^2 P_{mk}}{\partial t_{km}\partial \delta_m}\right]=-\frac{V_k V_m}{t_{km}}\left[-g_{mk}\sin\left(\delta_m-\delta_k\right)+b_{mk}\cos\left(\delta_m-\delta_k\right)\right]$$

$$\left[\frac{\partial^2 Q_m}{\partial t_{km}\partial V_k}\right]=\left[\frac{\partial^2 Q_{mk}}{\partial t_{km}\partial V_k}\right]=-\frac{V_m}{t_{km}}\left[-b_{mk}\cos\left(\delta_m-\delta_k\right)+g_{mk}\sin\left(\delta_m-\delta_k\right)\right]$$

$$\left[\frac{\partial^2 Q_m}{\partial t_{km}\partial V_m}\right]=\left[\frac{\partial^2 Q_{mk}}{\partial t_{km}\partial V_m}\right]=-\frac{1}{t_{km}}\left\{-4V_m b_{mm}+V_k\left[-b_{mk}\cos\left(\delta_m-\delta_k\right)+g_{mk}\sin\left(\delta_m-\delta_k\right)\right]\right\}$$

$$\left[\frac{\partial^2 Q_m}{\partial t_{km}\partial \delta_k}\right]=\left[\frac{\partial^2 Q_{mk}}{\partial t_{km}\partial \delta_k}\right]=-\frac{V_k V_m}{t_{km}}\left[-g_{mk}\cos\left(\delta_m-\delta_k\right)-b_{mk}\sin\left(\delta_m-\delta_k\right)\right]$$

$$\left[\frac{\partial^2 Q_m}{\partial t_{km}\partial \delta_m}\right]=\left[\frac{\partial^2 Q_{mk}}{\partial t_{km}\partial \delta_m}\right]=-\frac{V_k V_m}{t_{km}}\left[g_{mk}\cos\left(\delta_m-\delta_k\right)+b_{mk}\sin\left(\delta_m-\delta_k\right)\right]$$

$$\left[\frac{\partial\left|S_{km}\right|^2}{\partial t_{km}}\right]=2P_{km}\left[\frac{\partial P_{km}}{\partial t_{km}}\right]+2\mathrm{Q}_{km}\left[\frac{\partial \mathrm{Q}_{km}}{\partial t_{km}}\right]\quad \text{where } x = V_k, V_m, \delta_k, \text{ or } \delta_m$$

$$\left[\frac{\partial\left|S_{mk}\right|^2}{\partial t_{km}}\right]=2P_{mk}\left[\frac{\partial P_{mk}}{\partial t_{km}}\right]+2\mathrm{Q}_{mk}\left[\frac{\partial \mathrm{Q}_{mk}}{\partial t_{km}}\right]\quad \text{where } x = V_k, V_m, \delta_k, \text{ or } \delta_m$$

$$\left[\frac{\partial^2 |S_{km}|^2}{\partial t_{km}\partial x}\right] = 2P_{km}\left[\frac{\partial^2 P_{km}}{\partial t_{km}\partial x}\right] + 2\left[\frac{\partial P_{km}}{\partial x}\right]\left[\frac{\partial P_{km}}{\partial t_{km}}\right] + 2\mathrm{Q}_{km}\left[\frac{\partial^2 \mathrm{Q}_{km}}{\partial t_{km}\partial x}\right] + 2\left[\frac{\partial Q_{km}}{\partial x}\right]\left[\frac{\partial Q_{km}}{\partial t_{km}}\right]$$

where $x = V_k, V_m, \delta_k,$ or δ_m

$$\left[\frac{\partial^2 |S_{mk}|^2}{\partial t_{km}\partial x}\right] = 2P_{mk}\left[\frac{\partial^2 P_{mk}}{\partial t_{km}\partial x}\right] + 2\left[\frac{\partial P_{mk}}{\partial x}\right]\left[\frac{\partial P_{mk}}{\partial t_{km}}\right] + 2\mathrm{Q}_{mk}\left[\frac{\partial^2 \mathrm{Q}_{mk}}{\partial t_{km}\partial x}\right] + 2\left[\frac{\partial Q_{mk}}{\partial x}\right]\left[\frac{\partial Q_{mk}}{\partial t_{km}}\right]$$

where $x = V_k, V_m, \delta_k,$ or δ_m

Using the same process for phase shift angles, the following partial derivatives can be found.

$$\left[\frac{\partial P_k}{\partial \alpha_{km}}\right] = \left[\frac{\partial P_{km}}{\partial \alpha_{km}}\right] = V_k V_m\left[b_{km}\cos(\delta_k - \delta_m) - g_{km}\sin(\delta_k - \delta_m)\right]$$

$$\left[\frac{\partial Q_k}{\partial \alpha_{km}}\right] = \left[\frac{\partial Q_{km}}{\partial \alpha_{km}}\right] = V_k V_m\left[b_{km}\sin(\delta_k - \delta_m) + g_{km}\cos(\delta_k - \delta_m)\right]$$

$$\left[\frac{\partial P_m}{\partial \alpha_{km}}\right] = \left[\frac{\partial P_{mk}}{\partial \alpha_{km}}\right] = V_k V_m\left[-b_{mk}\cos(\delta_m - \delta_k) + g_{mk}\sin(\delta_m - \delta_k)\right]$$

$$\left[\frac{\partial Q_m}{\partial \alpha_{km}}\right] = \left[\frac{\partial Q_{mk}}{\partial \alpha_{km}}\right] = V_k V_m\left[-b_{mk}\sin(\delta_m - \delta_k) - g_{mk}\cos(\delta_m - \delta_k)\right]$$

$$\left[\frac{\partial^2 P_k}{\partial \alpha_{km}^2}\right] = \left[\frac{\partial^2 P_{km}}{\partial \alpha_{km}^2}\right] = -V_k V_m\left[g_{km}\cos(\delta_k - \delta_m) + b_{km}\sin(\delta_k - \delta_m)\right]$$

$$\left[\frac{\partial^2 Q_k}{\partial \alpha_{km}^2}\right] = \left[\frac{\partial^2 Q_{km}}{\partial \alpha_{km}^2}\right] = -V_k V_m\left[g_{km}\sin(\delta_k - \delta_m) - b_{km}\cos(\delta_k - \delta_m)\right]$$

$$\left[\frac{\partial^2 P_m}{\partial \alpha_{km}^2}\right] = \left[\frac{\partial^2 P_{mk}}{\partial \alpha_{km}^2}\right] = -V_k V_m\left[g_{mk}\cos(\delta_m - \delta_k) + b_{mk}\sin(\delta_m - \delta_k)\right]$$

$$\left[\frac{\partial^2 Q_m}{\partial \alpha_{km}^2}\right] = \left[\frac{\partial^2 Q_{mk}}{\partial \alpha_{km}^2}\right] = -V_k V_m\left[g_{mk}\sin(\delta_m - \delta_k) - b_{mk}\cos(\delta_m - \delta_k)\right]$$

$$\left[\frac{\partial^2 P_k}{\partial \alpha_{km}\partial V_k}\right]=\left[\frac{\partial^2 P_{km}}{\partial \alpha_{km}\partial V_k}\right]=V_m\left[b_{km}\cos\left(\delta_k-\delta_m\right)-g_{km}\sin\left(\delta_k-\delta_m\right)\right]$$

$$\left[\frac{\partial^2 P_k}{\partial \alpha_{km}\partial V_m}\right]=\left[\frac{\partial^2 P_{km}}{\partial \alpha_{km}\partial V_m}\right]=V_k\left[b_{km}\cos\left(\delta_k-\delta_m\right)-g_{km}\sin\left(\delta_k-\delta_m\right)\right]$$

$$\left[\frac{\partial^2 P_k}{\partial \alpha_{km}\partial \delta_k}\right]=\left[\frac{\partial^2 P_{km}}{\partial \alpha_{km}\partial \delta_k}\right]=V_kV_m\left[-b_{km}\sin\left(\delta_k-\delta_m\right)-g_{km}\cos\left(\delta_k-\delta_m\right)\right]$$

$$\left[\frac{\partial^2 P_k}{\partial \alpha_{km}\partial \delta_m}\right]=\left[\frac{\partial^2 P_{km}}{\partial \alpha_{km}\partial \delta_m}\right]=V_kV_m\left[b_{km}\sin\left(\delta_k-\delta_m\right)+g_{km}\cos\left(\delta_k-\delta_m\right)\right]$$

$$\left[\frac{\partial^2 Q_k}{\partial \alpha_{km}\partial V_k}\right]=\left[\frac{\partial^2 Q_{km}}{\partial \alpha_{km}\partial V_k}\right]=V_m\left[b_{km}\sin\left(\delta_k-\delta_m\right)+g_{km}\cos\left(\delta_k-\delta_m\right)\right]$$

$$\left[\frac{\partial^2 Q_k}{\partial \alpha_{km}\partial V_m}\right]=\left[\frac{\partial^2 Q_{km}}{\partial \alpha_{km}\partial V_m}\right]=V_k\left[b_{km}\sin\left(\delta_k-\delta_m\right)+g_{km}\cos\left(\delta_k-\delta_m\right)\right]$$

$$\left[\frac{\partial^2 Q_k}{\partial \alpha_{km}\partial \delta_k}\right]=\left[\frac{\partial^2 Q_{km}}{\partial \alpha_{km}\partial \delta_k}\right]=V_kV_m\left[b_{km}\cos\left(\delta_k-\delta_m\right)-g_{km}\sin\left(\delta_k-\delta_m\right)\right]$$

$$\left[\frac{\partial^2 Q_k}{\partial \alpha_{km}\partial \delta_m}\right]=\left[\frac{\partial^2 Q_{km}}{\partial \alpha_{km}\partial \delta_m}\right]=V_kV_m\left[-b_{km}\cos\left(\delta_k-\delta_m\right)+g_{km}\sin\left(\delta_k-\delta_m\right)\right]$$

$$\left[\frac{\partial^2 P_m}{\partial \alpha_{km}\partial V_k}\right]=\left[\frac{\partial^2 P_{mk}}{\partial \alpha_{km}\partial V_k}\right]=V_m\left[-b_{mk}\cos\left(\delta_m-\delta_k\right)+g_{mk}\sin\left(\delta_m-\delta_k\right)\right]$$

$$\left[\frac{\partial^2 P_m}{\partial \alpha_{km}\partial V_m}\right]=\left[\frac{\partial^2 P_{mk}}{\partial \alpha_{km}\partial V_m}\right]=V_k\left[-b_{mk}\cos\left(\delta_m-\delta_k\right)+g_{mk}\sin\left(\delta_m-\delta_k\right)\right]$$

$$\left[\frac{\partial^2 P_m}{\partial \alpha_{km}\partial \delta_k}\right]=\left[\frac{\partial^2 P_{mk}}{\partial \alpha_{km}\partial \delta_k}\right]=V_kV_m\left[-b_{mk}\sin\left(\delta_m-\delta_k\right)-g_{mk}\cos\left(\delta_m-\delta_k\right)\right]$$

$$\left[\frac{\partial^2 P_m}{\partial \alpha_{km}\partial \delta_m}\right]=\left[\frac{\partial^2 P_{mk}}{\partial \alpha_{km}\partial \delta_m}\right]=V_kV_m\left[b_{mk}\sin\left(\delta_m-\delta_k\right)+g_{mk}\cos\left(\delta_m-\delta_k\right)\right]$$

$$\left[\frac{\partial^2 Q_m}{\partial \alpha_{km}\partial V_k}\right]=\left[\frac{\partial^2 Q_{mk}}{\partial \alpha_{km}\partial V_k}\right]=V_m\left[-b_{mk}\sin\left(\delta_m-\delta_k\right)-g_{mk}\cos\left(\delta_m-\delta_k\right)\right]$$

$$\left[\frac{\partial^2 Q_m}{\partial \alpha_{km}\partial V_k}\right]=\left[\frac{\partial^2 Q_{mk}}{\partial \alpha_{km}\partial V_k}\right]=V_k\left[-b_{mk}\sin\left(\delta_m-\delta_k\right)-g_{mk}\cos\left(\delta_m-\delta_k\right)\right]$$

$$\left[\frac{\partial^2 Q_m}{\partial \alpha_{km}\partial \delta_k}\right]=\left[\frac{\partial^2 Q_{mk}}{\partial \alpha_{km}\partial \delta_k}\right]=V_kV_m\left[b_{mk}\cos\left(\delta_m-\delta_k\right)-g_{mk}\sin\left(\delta_m-\delta_k\right)\right]$$

$$\left[\frac{\partial^2 Q_m}{\partial \alpha_{km}\partial \delta_m}\right]=\left[\frac{\partial^2 Q_{mk}}{\partial \alpha_{km}\partial \delta_m}\right]=V_kV_m\left[-b_{mk}\cos\left(\delta_m-\delta_k\right)+g_{mk}\sin\left(\delta_m-\delta_k\right)\right]$$

$$\left[\frac{\partial\left|S_{km}\right|^2}{\partial \alpha_{km}}\right]=2P_{km}\left[\frac{\partial P_{km}}{\partial \alpha_{km}}\right]+2\mathrm{Q}_{km}\left[\frac{\partial \mathrm{Q}_{km}}{\partial \alpha_{km}}\right]\quad\text{where } x = V_k, V_m, \delta_k, \text{ or } \delta_m$$

$$\left[\frac{\partial\left|S_{mk}\right|^2}{\partial \alpha_{km}}\right]=2P_{mk}\left[\frac{\partial P_{mk}}{\partial \alpha_{km}}\right]+2\mathrm{Q}_{mk}\left[\frac{\partial \mathrm{Q}_{mk}}{\partial \alpha_{km}}\right]\quad\text{where } x = V_k, V_m, \delta_k, \text{ or } \delta_m$$

$$\left[\frac{\partial^2\left|S_{km}\right|^2}{\partial \alpha_{km}\partial x}\right]=2P_{km}\left[\frac{\partial^2 P_{km}}{\partial \alpha_{km}\partial x}\right]+2\left[\frac{\partial P_{km}}{\partial x}\right]\left[\frac{\partial P_{km}}{\partial \alpha_{km}}\right]+2\mathrm{Q}_{km}\left[\frac{\partial^2 \mathrm{Q}_{km}}{\partial \alpha_{km}\partial x}\right]+2\left[\frac{\partial Q_{km}}{\partial x}\right]\left[\frac{\partial Q_{km}}{\partial \alpha_{km}}\right]$$

where $x = V_k, V_m, \delta_k, \text{ or } \delta_m$

$$\left[\frac{\partial^2\left|S_{mk}\right|^2}{\partial \alpha_{km}\partial x}\right]=2P_{mk}\left[\frac{\partial^2 P_{mk}}{\partial \alpha_{km}\partial x}\right]+2\left[\frac{\partial P_{mk}}{\partial x}\right]\left[\frac{\partial P_{mk}}{\partial \alpha_{km}}\right]+2\mathrm{Q}_{mk}\left[\frac{\partial^2 \mathrm{Q}_{mk}}{\partial \alpha_{km}\partial x}\right]+2\left[\frac{\partial Q_{mk}}{\partial x}\right]\left[\frac{\partial Q_{mk}}{\partial \alpha_{km}}\right]$$

where $x = V_k, V_m, \delta_k, \text{ or } \delta_m$

APPENDIX E. SIX-BUS SAMPLE POWER SYSTEM

Appendix E contains information on the six-bus sample power system discussed in the thesis. A one-line diagram of the system is shown in Figure E.1.

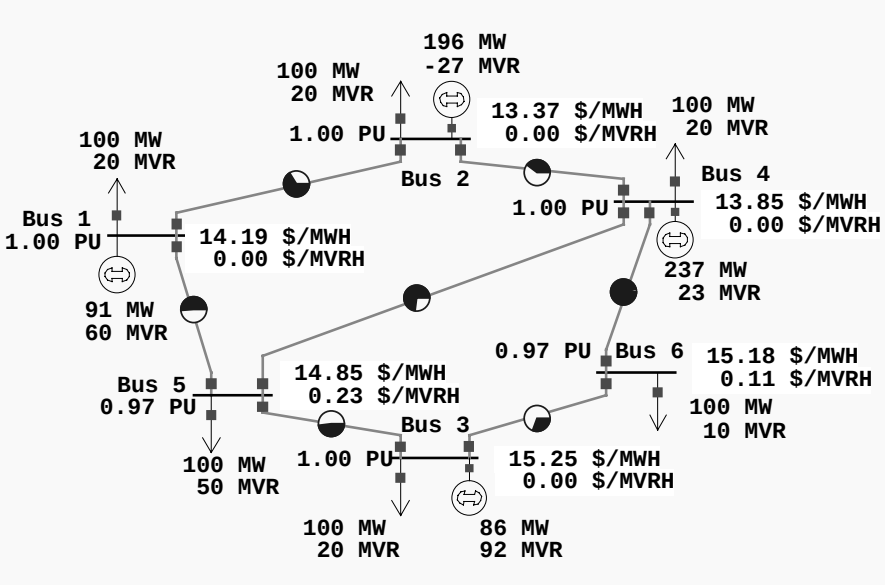

Figure E.1 One-Line Diagram of Six-Bus System

The line characteristics of the system are shown in Table E.1. The bus characteristics of the system are shown in Table E.2. The economic information of the system is shown in Table E.3.

Table E.1 Line characteristics for six-bus system

From Bus	To Bus	Circuit	Resistance [p.u.]	Reactance [p.u.]	Line Charging [p.u.]	Line Limit [MVA]
1	2	1	0.04	0.08	0.02	100
1	5	1	0.04	0.08	0.02	100
2	4	1	0.04	0.08	0.02	100
3	5	1	0.04	0.08	0.02	100
3	6	1	0.04	0.08	0.02	100
4	5	1	0.04	0.08	0.02	50
4	6	1	0.04	0.08	0.02	100

Table E.2 Bus characteristics for six-bus system

Bus Number	Load [MW]	Load [MVAR]	Min Generation [MW]	Max Generation [MVAR]
1	100	20	50	250
2	100	20	50	250
3	100	20	50	250
4	100	20	50	250
5	100	50	0	0
6	100	10	0	0

Table E.3 Economic information for six-bus system

Generator Bus	a $\left[\frac{\$}{\text{hr}}\right]$	b $\left[\frac{\$}{\text{MW hr}}\right]$	c $\left[\frac{\$}{\text{MW}^2\ \text{hr}}\right]$
1	105	12.0	0.0120
2	96	9.6	0.0096
3	105	13.0	0.0130
4	94	9.4	0.0094

APPENDIX F. TWENTY-THREE BUS SAMPLE POWER SYSTEM

Appendix F contains information on the twenty-three bus sample power system discussed in the thesis. A one-line diagram of the system is shown in Figure F.1.

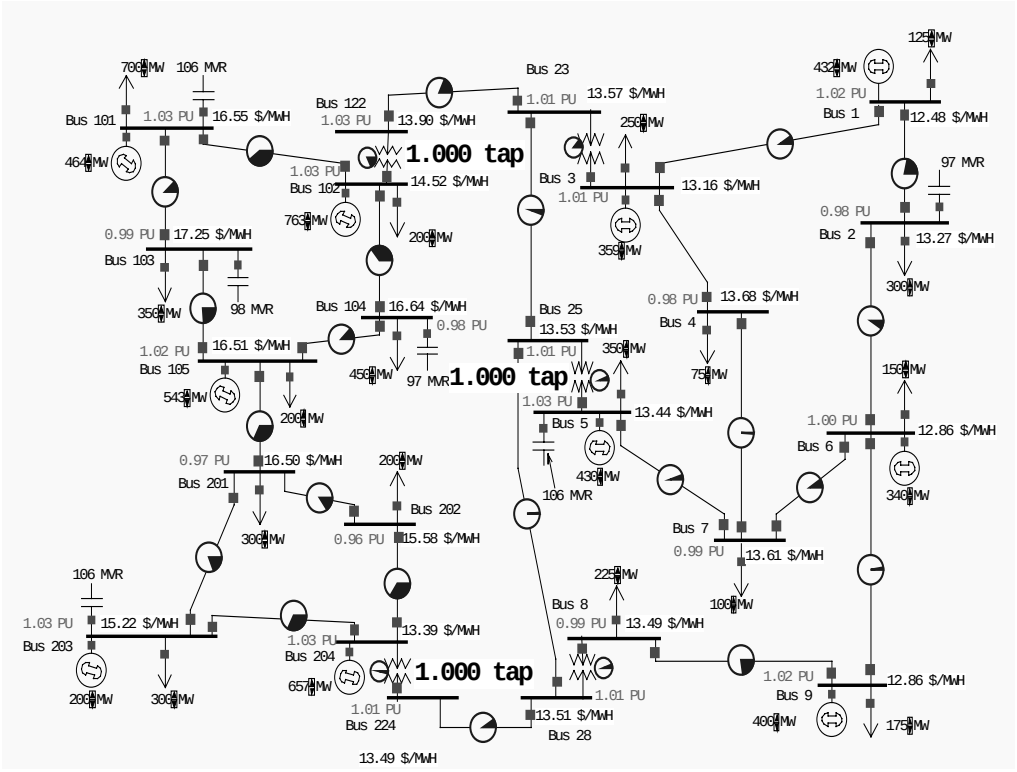

Figure F.1 One-Line Diagram of the Twenty-Three Bus System

The line characteristics of the system are shown in Table F.1. The bus characteristics of the system are shown in Table F.2. The economic information of the system is shown in Table F.3.

Table F.1 Line characteristics for twenty-three bus system

From Bus	To Bus	Circuit	Resistance [p.u.]	Reactance [p.u.]	Line Charging [p.u.]	Line Limit [MVA]
1	2	1	0.015	0.040	0.0005	1000
3	23	1	0.010	0.050	0.0000	1000
6	7	1	0.030	0.070	0.0000	1000
6	9	1	0.000	0.100	0.0000	1000
2	6	1	0.015	0.040	0.0006	1000
8	9	1	0.010	0.030	0.0050	1000
5	7	1	0.030	0.070	0.0000	1000
4	7	1	0.020	0.100	0.0005	1000
3	4	1	0.030	0.100	0.0000	1000
1	3	1	0.025	0.060	0.0005	1000
8	28	1	0.010	0.050	0.0000	1000
25	28	1	0.002	0.009	0.0008	1000
23	25	1	0.002	0.009	0.0008	1000
5	25	1	0.010	0.050	0.0000	1000
102	122	1	0.010	0.050	0.0000	1000
122	23	1	0.000	0.100	0.0000	1000
204	224	1	0.010	0.050	0.0000	1000
224	28	1	0.001	0.007	0.0005	500
105	201	1	0.010	0.030	0.0005	500
201	203	1	0.020	0.060	0.0005	1000
203	204	1	0.020	0.060	0.0000	1000
202	204	1	0.020	0.060	0.0000	1000
201	202	1	0.020	0.050	0.0005	1000
102	101	1	0.020	0.060	0.0000	1000
102	104	1	0.015	0.040	0.0008	1000
104	105	1	0.020	0.060	0.0005	1000
101	103	1	0.030	0.070	0.0000	1000
103	105	1	0.000	0.100	0.0000	1000

Table F.2 Bus characteristics for twenty-three bus system

Bus Number	Load [MW]	Load [MVAR]	Min Generation [MW]	Max Generation [MW]
1	125	50	100	1000
2	300	100	0	0
3	250	50	100	600
4	75	10	0	0
5	350	100	150	1000
6	150	35	100	400
7	100	10	0	0
8	225	75	0	0
9	175	50	100	800
23	0	0	0	0
25	0	0	0	0
28	0	0	0	0
101	700	200	100	600
102	200	20	200	1000
103	350	100	0	0
104	450	75	0	0
105	200	20	100	600
122	0	0	0	0
201	300	100	0	0
202	200	20	0	0
203	300	100	50	200
204	0	0	100	800
224	0	0	0	0

Table F.3 Economic information for six-bus system

Generator Bus	a $\left[\frac{\$}{\text{hr}}\right]$	b $\left[\frac{\$}{\text{MW hr}}\right]$	c $\left[\frac{\$}{\text{MW}^2\ \text{hr}}\right]$
1	55.43	7.9181	0.005279
3	58.90	7.6570	0.007657
5	64.28	7.7141	0.006428
6	58.90	7.6570	0.007657
9	80.47	7.5102	0.006897
101	72.94	7.2937	0.009981
102	74.24	7.8609	0.004367
105	65.59	7.5255	0.008285
203	65.91	7.5330	0.008161
204	70.81	7.9140	0.004165

APPENDIX G. SEVEN-BUS SAMPLE POWER SYSTEM

Appendix G contains information on the twenty-three bus sample power system discussed in the thesis. A one-line diagram of the system is shown in Figure G.1.

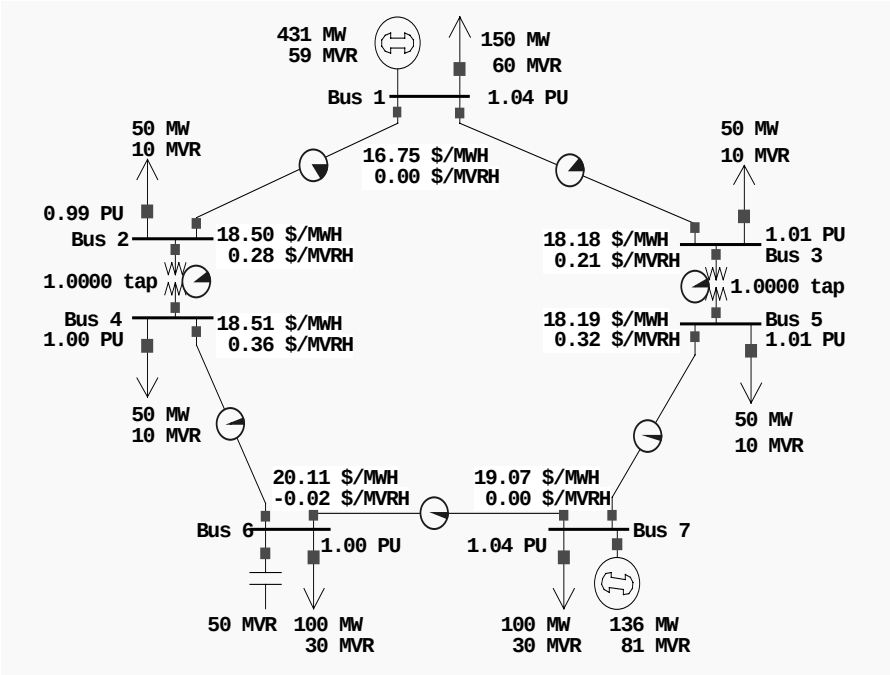

Figure G.1 One-Line Diagram of the Seven-Bus System

The line characteristics of the system are shown in Table G.1. The bus characteristics of the system are shown in Table G.2. The economic information of the system is shown in Table G.3.

Table G.1 Line characteristics for seven-bus system

From Bus	To Bus	R [p.u.]	X [p.u.]	C [p.u.]	Limit [MVA]
1	3	0.03	0.05	0.00	1000
2	1	0.03	0.05	0.00	1000
2*	4*	0.00	0.02	0.00	1000
3*	5*	0.11	0.02	0.00	1000
4	6	0.07	0.01	0.00	1000
6	7	0.06	0.10	0.00	1000
7	5	0.07	0.11	0.00	1000

* Note: Elements from buses 2-4 and 3-5 are transformers with tap ranges of 0.9 - 1.1 p.u.

Table G.2 Bus characteristics for seven-bus system

Bus Number	Load [MW]	Load [MVAR]	Min Gen. [MW]	Max Gen. [MW]
1	150	60	0	1000
2	50	10	0	0
3	50	10	0	0
4	50	10	0	0
5	50	10	0	0
6*	100	30	0	0
7	100	30	0	1000

* A 50 MVAR capacitor bank is at bus 6

Table G.3 Economic information for seven-bus system

Generator Bus	a $\left[\frac{\$}{\text{hr}}\right]$	b $\left[\frac{\$}{\text{MW hr}}\right]$	c $\left[\frac{\$}{\text{MW}^2\text{ hr}}\right]$
1	90	9.0	0.0090
7	115	15.0	0.0150

APPENDIX H. THREE-BUS SAMPLE POWER SYSTEM

Appendix H contains information on the twenty-three bus sample power system discussed in the thesis. A one-line diagram of the system is shown in Figure H.1.

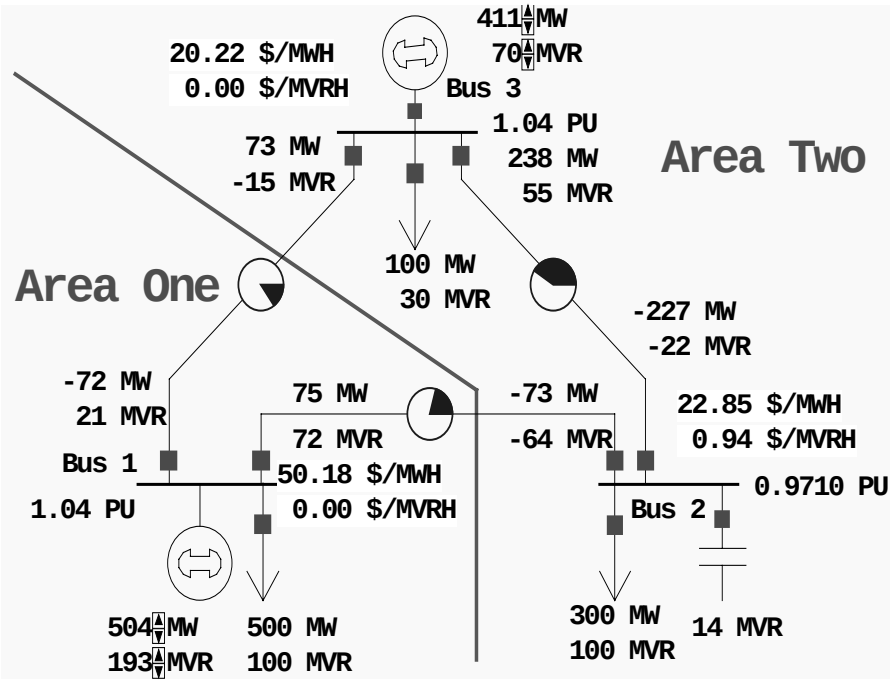

Figure H.1 One-Line Diagram of the Three-Bus System

The line characteristics of the system are shown in Table H.1. The bus characteristics of the system are shown in Table H.2. The economic information of the system is shown in Table H.3.

Table H.1 Line characteristics for three-bus system

From Bus	To Bus	R [p.u.]	X [p.u.]	C [p.u.]	Limit [MVA]
1	2	0.02	0.08	0.00	500
1	3	0.03	0.12	0.00	500
2	3	0.02	0.06	0.00	600

Table H.2 Bus characteristics for three-bus system

Bus Number	Load [MW]	Load [MVAR]	Min Gen. [MW]	Max Gen. [MW]
1	500	100	100	800
2	300	100	0	0
3	100	30	100	800

Table H.3 Economic information for three-bus system

Generator Bus	a $\left[\frac{\$}{\text{hr}}\right]$	b $\left[\frac{\$}{\text{MW hr}}\right]$	c $\left[\frac{\$}{\text{MW}^2\ \text{hr}}\right]$
1	100	25.0	0.0250
3	150	13.0	0.0100

REFERENCES

[1] S. Hunt and G. Shuttleworth, "Unlocking the GRID," *IEEE Spectrum*, Vol. 33, No. 7, July 1996, pp. 20-25.

[2] B. R. Barkovich and D. Hawk, "Charting a new course in California," *IEEE Spectrum*, Vol. 33, No. 7, July 1996, pp. 26-31.

[3] M. G. Morgan and S. Talukdar, "Nurturing R&D," *IEEE Spectrum*, Vol. 33, No. 7, July 1996, pp. 32,33.

[4] H. Rudnick, "Pioneering electricity reform in South America," *IEEE Spectrum*, Vol. 33, No. 8, August 1996, p. 38-44.

[5] R. D. Tabors, "Lessons from the UK and Norway," *IEEE Spectrum*, Vol. 33, No. 8, August 1996, pp. 45-49.

[6] R. D. Masiello, "It's put up or shut up for grid controls," *IEEE Spectrum*, Vol. 33, No. 8, August 1996, pp. 50,51.

[7] Federal Energy Regulatory Commission of the United States of America, "Promoting wholesale competition through open access non-discriminatory transmission services by public utilities," Docket No. RM95-8-00, March 1995.

[8] "WSCC Unfolds Causes of the July 2 Disturbance," *IEEE Power Engineering Review*, Vol. 16, No. 9, September 1996, pp. 5,6.

[9] The joint PSERC/EPRI workshop on underlying technical issues in electricity deregulation, Tucson, Arizona, April 25-27, 1996.

[10] J. Carpienter, "Contribution e l'étude do Dispatching Economique," *Bulletin Society Française Electriciens*, Vol. 3, August 1962.

[11] A. J. Wood and B. F. Wollenberg, *Power Generation Operation and Control*, New York, NY: John Wiley & Sons, Inc., 1996, pp. 39,517.

[12] H. W. Dommel and W. F. Tinney, "Optimal Power Flow Solutions," *IEEE Transactions on Power Apparatus and Systems*, Vol. PAS-87, October 1968, pp. 1866-1876.

[13] D. I. Sun, B. Ashley, B. Brewer, A. Hughes and W. F. Tinney, "Optimal Power Flow by Newton Approach," *IEEE Transactions on Power Apparatus and Systems*, Vol. PAS-103, October 1984, pp. 2864-2880.

[14] O. Alsac, J. Bright, M. Prais and B. Stott, "Further Developments in LP-Based Optimal Power Flow," *IEEE Transactions on Power Systems*, Vol. 5, No. 3, August 1990, pp. 697-711.

[15] Y. Wu, A. S. Debs and R. E. Marsten, "Direct Nonlinear Predictor-Corrector Primal-Dual Interior Point Algorithm for Optimal Power Flows," *1993 IEEE Power Industry Computer Applications Conference*, pp. 138-145.

[16] M. Huneault and F. D. Galiana, "A Survey of the Optimal Power Flow Literature," *IEEE Transactions on Power Systems*, Vol. 6, No. 2, May 1991, pp. 762-770.

[17] T. J. Overbye, P. W. Sauer, C. M. Marzinzik and G. Gross, "A User-Friendly Simulation Program for Teaching Power System Operations," *IEEE Transactions on Power Systems*, Vol. 10, No. 4, November 1995, pp. 1725-1733.

[18] W. F. Tinney and C. E. Hart, "Power Flow Solution by Newton's Method," *IEEE Transactions on Power Apparatus and Systems*, Vol. PAS-86, No. 11, November 1967, pp. 1866-1876.

[19] D. G. Luenberger, *Linear and Non-Linear Programming*, Reading, MA: Addison-Wesley Publishing Company, 1984, pp. 295-392,423-450.

[20] J. J. Grainger and W. D. Stevenson, *Power System Analysis*, New York, NY: McGraw Hill, Inc., 1994, pp. 33,330.

[21] E. Liu, A. D. Papalexopoulos and W. F. Tinney, "Discrete Shunt Controls in A Newton Optimal Power Flow," *IEEE Transactions on Power Systems*, Vol. 7, No. 4, November 1992, pp. 1519-1528.

[22] J. A. Momah, R. J. Koessler, M. S. Bond, B. Stott, D. Sun, A. D. Papalexopoulos and P. Ristanovic, "Challenges to Optimal Power Flow," *1996 IEEE/PES Winter Meeting*, 96 WM 312-9 PWRS, January 21-25, 1996, Baltimore, MD.

[23] C.A. Gross, *Power System Analysis*, New York, NY: John Wiley & Sons, Inc., 1979.

[24] G. E. Forsythe and C. B. Moler, *Computer Solution of Linear Algebraic Systems*, Englewood Cliffs, N.J.: Prentice-Hall, 1967, Chapters 9 and 16.

[25] S. M. Chan and V. Brandwajn, "Partial Matrix Refactorization," *IEEE Transactions on Power Systems*, Vol. PWRS-1, No. 1, February 1986, pp. 193-200.

[26] J. D. Weber, M. J. Laufenberg, T. J. Overbye and P. W. Sauer, "Assessing the Value of Reactive Power Services in Electric Power Systems," Conference on Unbundled Power Quality Services, Key West, Florida, November 17-19, 1996.

[27] R. D. Tabors, “Transmission System Management and Pricing: New Paradigms and International Comparisons,” *IEEE Transactions on Power Systems*, Vol. 9, No. 1, February 1994, pp. 206-215.

[28] D. Shirmohammadi, X.V. Filho, B. Gorenstin and M. Pereira, “Some fundamental technical concepts about cost based transmission pricing,” *IEEE Transactions on Power Systems*, Vol. 11, No. 2, May 1996, pp. 1002-1008.

[29] D. A. Wismer and R. Chattergy, *Introduction to Non-Linear Optimization, A Problem Solving Approach*, New York, NY: North Holland Publishing, 1978.